Chinese Journal of
POLYMER SCIENCE

REVIEW

https://doi.org/10.1007/s10118-026-3578-9
Chinese J. Polym. Sci. **2026**, *44*, 1695–1715

Engineering Hydrogel-based Self-floating Catalytic Materials for Interfacial Solar-driven Chemistry

Jia-Xin Gao and Wen-Wei Lei*

School of Environmental and Chemical Engineering, State Key Laboratory of Metastable Materials Science and Technology, Hebei Key Laboratory of Nanobiotechnology, Yanshan University, Qinhuangdao 066004, China

Abstract Hydrogel-based self-floating catalytic materials have become a key interfacial platform in the field of solar-driven chemistry, effectively solving the difficulties of traditional powder catalysts in the aqueous phase, such as easy agglomeration, sedimentation, and limited mass transfer. In this study, the design strategy, structural properties, and interfacial advantages of these materials were systematically described, and the mechanisms of precursor mixing, *in situ* synthesis, and post-modification in regulating the distribution of active sites, gel structure formation, and multifunctional integration were analyzed. Through the construction of stable three-phase interfaces, the materials form a reaction microenvironment with a generalized enhancement effect. The structural design significantly improves the light trapping efficiency and carrier separation performance in photocatalytic processes and simultaneously strengthens the mass transfer process and local reactant concentration in peroxide activation reactions, establishing a synergistic system in which the adsorption, enrichment, and catalytic processes are tightly coupled. Successful applications in the fields of organic pollutant degradation, solar-driven chemical synthesis, and interfacial evaporation have demonstrated the wide applicability of this technology. By systematically combining the research progress in this field, this study aims to provide a theoretical basis for the development of efficient and stable interfacial catalytic platforms and promote the development of sustainable environmental remediation and energy conversion technologies.

Keywords Self-floating; Hydrogel-based catalyst; Three-phase interface; Construction strategies; Multifunctional application

Citation: Gao, J. X.; Lei, W. W. Engineering hydrogel-based self-floating catalytic materials for interfacial solar-driven chemistry. *Chinese J. Polym. Sci.* **2026**, *44*, 1695–1715.

INTRODUCTION

Solar-driven chemical processes are key to addressing the dual challenges of environmental remediation and sustainable energy conversion.[1–5] Such processes rely on photo-stimulated redox reactions for pollutant degradation or fuel synthesis, and their efficiencies are largely limited by the performance of the heterogeneous catalysts. Heterogeneous catalysis plays a significant role in water pollution control, energy conversion, and environmental remediation, and its efficiency is highly dependent on the effective interfacial contact between the catalyst and reactants and the mass transfer process.[6–10] Nano-scale catalysts have high specific surface areas, but they easily agglomerate in the liquid phase, which not only reduces the availability of active sites but also may lead to secondary pollution. At the same time, the long-range diffusion of the reactants in the bulk solution restricts them from approaching the active center, which leads to a decrease in mass-transfer efficiency, especially at low pollutant concentrations. In addition, in light-driven systems, such as photocatalysis or photothermal catalysis, the catalyst dispersed in the water body greatly weakens the efficiency of photon utilization owing to the light absorption and scattering effect of water, thus restricting the overall energy conversion efficiency.

To overcome these limitations, interface-confined catalytic techniques have emerged as a revolutionary strategy.[11–14] Among them, catalysts capable of spontaneously floating at the gas-water interface exhibit unique potential because of their ability to establish a stable three-phase reaction zone.[15–19] Ideal floating platforms need to be lightweight, porous, mechanically strong, and firmly loaded with various catalytically active components. However, existing floating materials (*e.g.*, polymer foams,[20–23] carbon-based materials,[24,25] wood substrates,[26–28] and aerogels[29,30]) still have deficiencies in structural controllability, functional integration, and long-term stability, which limit their practical applications in complex interfacial reaction systems.

Thanks to their three-dimensional cross-linked networks and hierarchical pore structures rich in surface functional groups,[6,31–34] hydrogels can provide highly dispersed and stable anchoring sites for metal nanoparticles, metal oxides/sulfides,[35–38] single-atom centers,[39–41] and molecular catalysts.[42–44] Meanwhile, the density and surface wettability of hydrogels can be precisely regulated by freeze-drying, foaming strategy, or hydrophobic modification to

* Corresponding author, E-mail: leiww@ysu.edu.cn
Special Topic: Functional Gels
Received December 29, 2025; Accepted January 14, 2026; Published online May 12, 2026

© Chinese Chemical Society
Institute of Chemistry, Chinese Academy of Sciences

achieve long-term self-floating performance. Benefiting from these structural tunabilities, the past five years have witnessed a rapid expansion of hydrogel-based self-floating catalytic systems driven by advances in gel engineering, interfacial design, and solar-driven reaction platforms, which has led to a surge of high-quality studies and increasingly diversified application scenarios.[34,39,43–47] The incorporation of photothermal materials, conductive polymers, or functional monomers with tunable coordination structures can further enhance the light absorption, interfacial reactivity, and mass transfer capabilities of the materials to achieve integrated and efficient multifunctional performance. In particular, the three-phase interface constructed using the floating hydrogel exerts a universal reaction-enhancing effect. This effect not only maximizes the light-trapping efficiency for photocatalytic and photothermal processes, but also creates a highly concentrated microenvironment for peroxide-activated oxidative reactions, such as the Fenton reaction and advanced oxidation processes (AOPs), through the simultaneous enrichment of catalysts, pollutants, and oxidants.

Although recent reviews have discussed floating photocatalysts, floatable hydrogels, or interfacial solar evaporation systems, this study uniquely focuses on hydrogel-based self-floating catalysts as a unifying platform for interfacial solar energy-driven chemistry. Through careful analysis of material construction methods, three-phase interfacial mechanisms, and multifunctional catalytic and energy conversion behaviors, this review seeks to elucidate the relationship between structure, interface, and function, highlighting the unique capabilities of these systems for pollution mitigation and sustainable energy use under complex environmental conditions.

In particular, this paper provides a comprehensive overview of advances in structural design, floating mechanisms, and interfacial catalytic properties, focusing on representative applications, such as organic pollutant degradation, solar-powered energy and resource conversion, and integrated desalination (Fig. 1). By synthesizing and critically examining existing studies, we aim to provide a solid theoretical foundation and practical guidance for the optimization and implementation of hydrogel-based self-floating catalytic systems in real-world applications.

OVERVIEW OF HYDROGEL-BASED SELF-FLOATING CATALYTIC MATERIALS

Hydrogel-based self-floating catalytic materials are an emerging class of interfacial catalytic platforms that derive their performance advantages from their precisely tunable multiscale structures and significant enhancement of interfacial reaction processes.[48,49] In-depth understanding of the structure formation principle and key properties is of great significance for optimizing the performance and expanding the practical applications of these materials.

Structural Design Strategies and Floating Mechanisms

The excellent performance of hydrogel-based self-floating catalysts stems from the synergistic integration of two core elements: the catalytic functional structure design of the gel matrix and the engineering regulation of the floating behavior. In material preparation, the two are often synchronized and mutually reinforced.

Catalytic activity mainly depends on the chemical composition and porous structure of the hydrogel. The matrix is a three-dimensional cross-linked hydrophilic polymer network that can be modified by selecting specific monomers (acrylamide, sodium alginate, and acrylic acid), cross-linking agents (*N*,*N*'-methylene bis acrylamide, multivalent metal ions), and functional groups (—OH, —COOH, —NH_2, —$CONH_2$),[50–54] which can precisely regulate the chemical composition and network structure, thus providing uniform and stable anchor sites for catalytically active components through liganding, hydrogen bonding, or electrostatic interactions and effectively preventing the deactivation of ag-

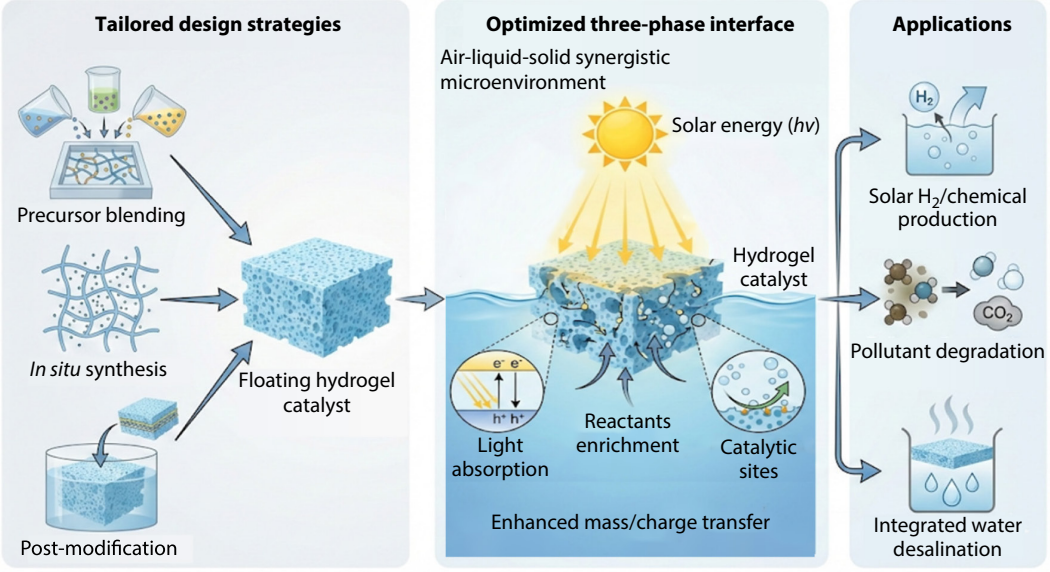

Fig. 1 Schematic illustration of the construction strategies and main applications of hydrogel-based self-floating catalytic materials.

glomerates.[55]

Simultaneously, the construction of coherent and hierarchical pore structures is crucial for realizing efficient mass transfer. Macropores (>100 nm) promote overall fluid flow, mesopores (2–100 nm) provide a high specific surface area, and micropores (<2 nm) facilitate small-molecule enrichment. Such multistage pores can be introduced during the gelation process or its later stages by techniques such as ice templating (freeze-drying), sacrificial templating (salt particles or polymer microspheres), or *in situ* foaming,[56–59] which can efficiently shorten the reactant diffusion paths and alleviate the mass transfer limitations that are common in conventional systems.

The key to achieving spontaneous and stable floating lies in the balance between the density and surface wettability. Reducing the density mainly relies on the introduction of a large number of pores in the gel matrix, which is consistent with the pore-making strategies described above (freeze-drying, gas foaming, salt particles, *etc.*), such that the density of the material is lower than that of water to generate buoyancy. In addition to the long-term floating of the gel material through a pore-making strategy, interface wettability regulation is also a key way to achieve this goal. By rationally designing the chemical composition and microstructure of the material surface, the interaction with the gas-liquid interface can be accurately regulated to achieve stable interfacial anchoring and floating state.[60–62] The intrinsic hydrophilicity of gels leads to water absorption and sinking, so hydrophobic modification of the surface or the whole is often required, such as the introduction of hydrophobic monomers, grafting of hydrophobic chains, or deposition of hydrophobic coatings. This modification leads to the formation of a stable Cassie-Baxter state at the interface, which traps air in the surface roughness structure, thus enhancing the resistance to perturbed drift. The establishment of an efficient three-phase reaction zone relies on the construction of a lightweight porous skeleton and modulation of the hydrophobic interface, both of which simultaneously guarantee that the material maintains a stable position at the gas-liquid boundary.[57,58]

Performance Advantages of Hydrogel-based Self-floating Catalytic Materials

Hydrogel-based self-floating catalytic materials exhibit obvious advantages over powder catalysts and common floating carriers by utilizing their designable network structure, graded pores, and unique interfacial behavior.[47,63–68] These advantages stem from the synergistic effects of active site dispersion, interfacial enrichment, mass transfer enhancement, and light utilization enhancement, which together promote a significant improvement in interfacial catalytic efficiency.

Although traditional powder catalysts have a high specific surface area, they are prone to agglomeration, sedimentation, and dissolution in aqueous environments, leading to a decrease in the accessibility of active sites and difficulties in recycling. In contrast, the three-dimensional crosslinked network of hydrogels is rich in hydrophilic functional groups such as —OH, —COOH, —$CONH_2$, which can securely fix metal ions, nanoparticles, and even single-atom centers through ligand, hydrogen bonding, or electrostatic interaction, forming a stable, uniform, and adjustable catalytic microenvironment, effectively inhibiting the migration, aggregation, and dissolution of active species. It can effectively inhibit the migration, aggregation, and dissolution of active species, thus enhancing structural stability and long-lasting catalytic performance.[69–73]

When designed as self-floating structures, hydrogels exhibit enhanced durability. As shown in Fig. 2, the floating state enables the material to be located at the gas-liquid interface instead of being completely submerged, which greatly reduces deactivation phenomena such as deposition, ion erosion, and surface blockage. Interfacial positioning also guarantees that the active centers are continuously exposed to light, avoiding the aggregation of photoactive sites caused by local overheating. As a result, the self-floating hydrogel showed better durability and operational stability than traditional powder or bulk catalysts in complex reaction environments.

Self-floating hydrogels can localize the catalyst at the air-water interface to construct a stable and efficient three-phase reaction zone.[46,57,58,74,75] As shown in Fig. 3, when the hydrogel floats on the water surface and is irradiated by light, the gas-phase reactants (O_2) can be directly transported to the active sites by air, while the water pollutants rapidly diffuse into the gel network and are selectively enriched in the porous matrix. The through graded pores shorten the diffusion path and reduce the mass transfer resistance, so that the reaction control is dominated by interfacial reactions instead

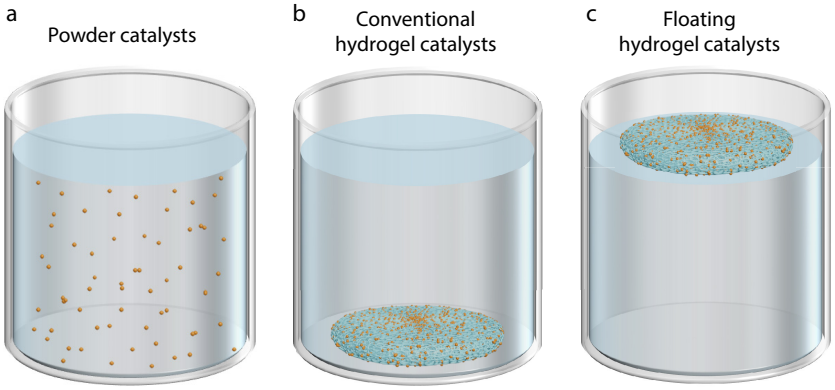

Fig. 2 Schematic illustration of the distribution states of (a) powder catalysts, (b) conventional and (c) self-floating hydrogel-based catalytic materials in water.

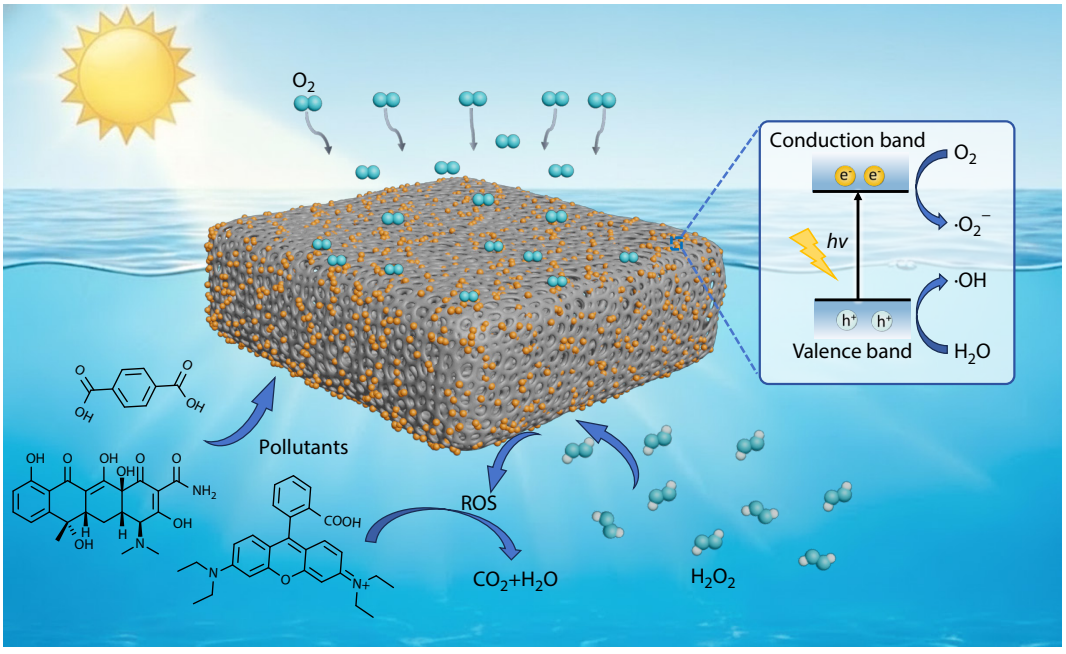

Fig. 3 Schematic illustration of the catalytic mechanism of hydrogel-based self-floating catalytic materials at the gas-liquid-solid interface. When floating on the water surface and exposed to light, the material enables efficient O_2 supply, pollutant adsorption, ROS generation, and pollutant degradation.

of bulk phase diffusion. The strong adsorption capacity of the hydrogel leads to the localized enrichment of pollutants in the vicinity of the active site, thus significantly increasing the concentration of reactants in the interfacial reaction zone and maintaining efficient reaction activity even under trace pollutant conditions.

Hydrogel-based self-floating catalytic systems can enhance various catalytic reactions. In solar-driven processes, direct exposure to incident light reduces scattering and absorption losses, whereas the enclosed hydrogel matrix promotes the separation of photogenerated carriers and improves the generation of reactive oxygen species (ROS). During peroxide-activated oxidation, hydrogels can simultaneously enrich gas-phase reactants, oxidants, and pollutants,[76–79] serving not only as a catalyst carrier but also as a multifunctional platform that integrates material enrichment, interfacial catalysis, and reaction enhancement.

CONSTRUCTION STRATEGIES

The construction of hydrogel-based self-floating catalytic materials needs to simultaneously satisfy three core objectives: (i) stable immobilization of catalytically active sites, (ii) formation of a lightweight porous gel skeleton, and (iii) long-term stable floating at the gas-water interface.[46,67,80] Three representative strategies (precursor mixing, *in situ* synthesis and post-modified loading) have been developed around these goals. The fundamental difference between these approaches lies in the timing and mode of catalyst introduction relative to the sequence of gel network formation, which directly affects catalyst dispersion, interfacial bonding strength, and structural tunability. Therefore, a brief review of the above three construction strategies will help lay the foundation for subsequent in-depth discussion.

Precursor Blending Approach for Integrating Catalytic Activity and Self-floating Structures

Precursor mixing is one of the most fundamental and widely used construction strategies for building hydrogel-based self-floating catalytic materials. At its core, polymer precursors, catalytically active components or their precursors, and functional additives for structure modulation are homogeneously mixed in a solvent before gelation. Subsequently, the embedding of the catalyst, formation of a three-dimensional network, and construction of the porous floating structure are synchronized through cross-linking and structure modulation steps. This method has been widely used for the preparation of floating hydrogel catalysts because of its clear preparation pathway, high material compatibility, and ability to maintain high catalytic activity and structural stability in a variety of systems.

In a typical preparation process, water-soluble or well-dispersible polymers (*e.g.*, poly(vinyl alcohol) (PVA), sodium alginate (SA), and cellulose derivatives) are first dissolved or dispersed in the aqueous phase to form a homogeneous precursor solution.[81] Subsequently, catalytically active substances (*e.g.*, metal oxides, metal (oxy)hydroxides, single-atom catalysts, and semiconductor nanomaterials) or functional nanofillers (*e.g.*, carbon materials, graphene derivatives, and MXenes) are introduced into the system, and homogeneous mixing is achieved by mechanical stirring, ultrasonic dispersion, or static diffusion. Guo *et al.* directly dispersed CuO and antimony-doped tin oxide (ATO) nanoparticles in a 5 wt% aqueous PVA solution, and a homogeneous mixture was obtained by magnetic stirring (Fig. 4a).[82] The good macroscopic mobility of the gel precursor solution at this stage ensures that the active components are uniformly distributed in the system, laying the foundation for the subsequent formation of highly dispersed and firmly fixed catalytic sites.

After homogenization of the precursor, a three-dimension-

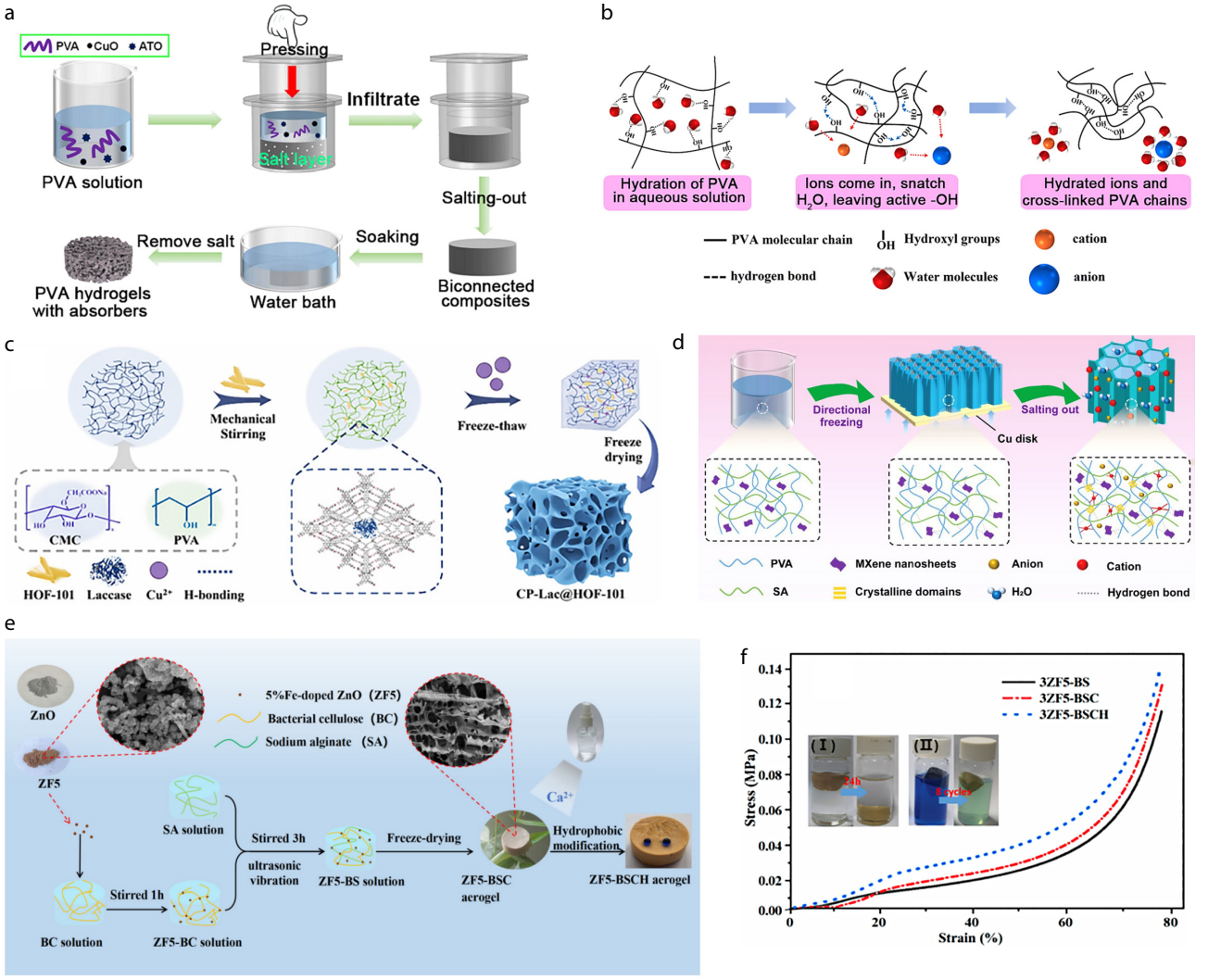

Fig. 4 (a) The preparation process following the salting-out/sacrificial template strategy; (b) The suggested mechanism of the salting-out/cross-linking process; (a, b: reproduced with permission from Ref. [82]; Copyright (2024), Elsevier.) (c) Schematic diagram of the preparation process of CP-Lac@HOF-101 (Reproduced with permission from Ref. [84]; Copyright (2023), Elsevier); (d) Schematic illustrating the fabrication process of PSMH (Reproduced with permission from Ref. [85]; Copyright (2024), American Chemical Society); (e) Preparation of ZF5-BSCH composite aerogel; (f) Compressive stress-strain curves of 3ZF5-BS, 3ZF5-BSC, and 3ZF5-BSCH, inset I: ZF5-BSCH after oscillating for 24 h, inset II: after 8 photocatalytic degradation cycles. (e, f: reproduced with permission from Ref. [86]; Copyright (2024), Springer Nature.)

al gel network formation is usually induced by physical or chemical cross-linking. Commonly used cross-linking methods include chemical cross-linking, freeze-thaw cross-linking and ionic cross-linking.[83] It is worth noting that the cross-linking process not only determines the mechanical strength and stability of the gel skeleton but also directly affects the immobilization pattern and spatial distribution of catalytically active substances. In precursor hybrid systems, the catalyst or its precursor is often confined *in situ* between polymer chain segments during network formation. This simultaneous formation mechanism effectively avoids the problems of catalyst detachment, migration or uneven distribution, which are common in post-modification or impregnation methods, and thus significantly improves the structural integrity and recyclability of the catalytic system.

In addition to the easy and efficient embedding of catalysts, the precursor mixing method offers a high degree of flexibility for the construction of porous structures and lightweight materials. With the help of sacrificial template or ice template strategies, pores on scales ranging from micrometers to hundreds of micrometers can be fabricated in gel networks. In the sacrificial template method, a prefabricated, selectively removable template phase is homogeneously dispersed in the gel precursor, after which the template is removed by dissolution, chemical etching, *etc.*, to replicate pore structures with specific morphologies and sizes. Guo *et al.* used a salt precipitation/artificial template strategy to induce PVA chain rearrangement and pore formation and successfully prepared a highly porous hydrogel with a microchannel structure and excellent durability.[82] As shown in Fig. 4(b), the PVA chains were initially uniformly dispersed through hydrogen bonding with water molecules, and upon contact with salt particles, the dissociative ions competed with the polymer chains for hydration molecules, stripping off the hydra-

tion layer of the PVA chains. The exposed —OH groups then reconfigured the inter-chain hydrogen bonding, which led to the solidification of the gel network and the simultaneous formation of the porous structure. This strategy endows the hydrogel with robust structural integrity and highly interconnected internal pores, which facilitate rapid transport of reactants and water.

Freeze-drying, the most representative ice template technology, is also widely used in precursor mixing systems. During the freezing process, ice crystals act as dynamic templates, crowding the polymer chains and catalytic components in the intergranular region, after ice sublimation, a highly interconnected penetration network is retained within the gel. Yang *et al.* prepared CMC/PVA/ Lac@HOF-101 hydrogels with a two-dimensional periodic "square lattice network" structure by combining freeze-thaw cycling with freeze-drying (Fig. 4c).[84] The Lac@HOF-101 hydrogel has a two-dimensional periodic "square lattice" structure. This porous structure significantly improves the internal transport of reactants and gases, while reducing the overall density of the material and realizing spontaneous floating.

To solve the problems of random pore orientation and slow solvent migration that may occur in conventional freeze-drying, directional freeze-casting technology was introduced. This technique induces the growth of ice crystals along a specific direction by establishing a unidirectional temperature gradient, which results in the formation of highly oriented pores. For example, Li *et al.* injected a homogeneous PVA/SA/MXene precursor solution into a polytetrafluoroethylene mold, the bottom of the mold was placed in contact with a liquid nitrogen-cooled copper plate to establish a unidirectional thermal gradient, and a PVA/SA/MXene hydrogel (PSMH) was obtained by freezing and ionic cross-linking (Fig. 4d). Scanning electron microscopy (SEM) images showed that PSMH has a vertically aligned channel structure with regularly distributed pores on the channel walls connecting neighboring channels to form a network of oriented and fully interpenetrating pores.[85]

Based on the above structural design, the mechanical stability of the gel skeleton can be further enhanced and its wettability can be regulated by secondary cross-linking or surface/interfacial hydrophobic modification, thus guaranteeing the long-term self-floating ability of the material under continuous operation. Zhang *et al.* adopted this strategy by first mixing the catalyst particles with gel precursors and then constructing a structure with a high specific surface area and high porosity by freeze-drying. Subsequently, a 2 wt% $CaCl_2$ ethanol solution was sprayed for secondary cross-linking to strengthen the skeleton, and hydrophobic modification was performed to enhance the floating stability of the water surface. Finally, Fe-doped ZnO/bacterial cellulose-based composite (ZF5-BSCH) aerogels were successfully prepared (Fig. 4e). After the secondary cross-linking, the mechanical properties of the ZF5-BSCH aerogel were significantly enhanced (Fig. 4f); it did not dissolve after 24 h under mechanical stirring at 200 r/min (inset I) and was able to maintain its structural integrity after eight rounds of photocatalytic reaction (inset II).[86] This stepwise functionalization design provides a scalable preparation pathway for the development of self-leaving catalytic materials with both high activity and high durability.

In situ Construction of Catalytic Active Sites and Floating Architectures within Gel-confined Environments

The *in situ* synthesis method is a pivotal strategy for the direct generation, immobilization, or chemical bonding of catalytically active components in hydrogel networks. Compared with other methods, this route exhibits significant structural and performance advantages in self-floating hydrogel catalytic systems, that is, it uses preformed or partially crosslinked hydrogel as a three-dimensional domain-limited reactor and makes full use of the gel's unique high porosity, continuous water channels, and abundant functional groups on the polymer chain, thus realizing efficient adsorption, uniform distribution, and controlled *in situ* conversion of catalyst precursors in the matrix.[50–54]

In situ reduction method

As one of the most widely used and mechanistically well-defined strategies in *in situ* synthesis, the *in situ* reduction method is mainly used to construct catalytically active centers of metal nanoparticles in gel networks. This method uses metal ions adsorbed in the gel matrix as precursors, which are gradually converted into zero-valent metal nanoparticles by external chemical reduction or physical reduction techniques under mild conditions.[36,87,88] Despite the differences in the specific reduction pathways, the core objective is to achieve slow and controlled nucleation and growth of metal species in the gel-limited space.

Lin *et al.* introduced a large number of bubbles by mechanical blending acrylamide (AM), graphene oxide (GO) and AgNO_3. Under γ-ray irradiation, polymerization of the PAM network was induced, GO was partially reduced, and Ag^+ was synchronized with *in situ* reduction, resulting in three-dimensional porous ArG-Ag hydrogels (Fig. 5a).[89] γ-Ray irradiation, as a means of physical reduction without a chemical reductant, has the advantages of homogeneous reduction, clean reaction, and controllable particle size, which are particularly suited to the construction of highly dispersed metal nanostructures. In contrast, the classical impregnation-chemical reduction pathway was employed by Nayak *et al.* As shown in Fig. 5(b), chitosan-graphene oxide (CSGO) gel is a three-dimensional adsorption scaffold for Ag^+, which enables the uniform adsorption of Ag^+ in the gel network. The subsequent introduction of $NaBH_4$ as a strong reducing agent can rapidly convert the adsorbed Ag^+ into well-dispersed Ag nanoparticles enclosed in the gel matrix, and a lightweight self-floating gel catalyst with fixed metal active sites was obtained by freeze-drying.[90] It can be seen that through the three-dimensional domain-limiting effect and functional group anchoring effect of hydrogels, the *in situ* reduction method realizes the controllable formation, homogeneous dispersion and stable solidification of metal nanoparticles, which becomes an important basic strategy for the construction of self-floating metal-based hydrogel catalysts.

In situ precipitation and transformation methods

The *in situ* precipitation method relies on inducing the nucleation and growth of metal compounds in the domain-limited space of the gel to construct catalytically active components, and thus is particularly suitable for combining the adsorption properties of hydrogels with their catalytic functions.

https://doi.org/10.1007/s10118-026-3578-9

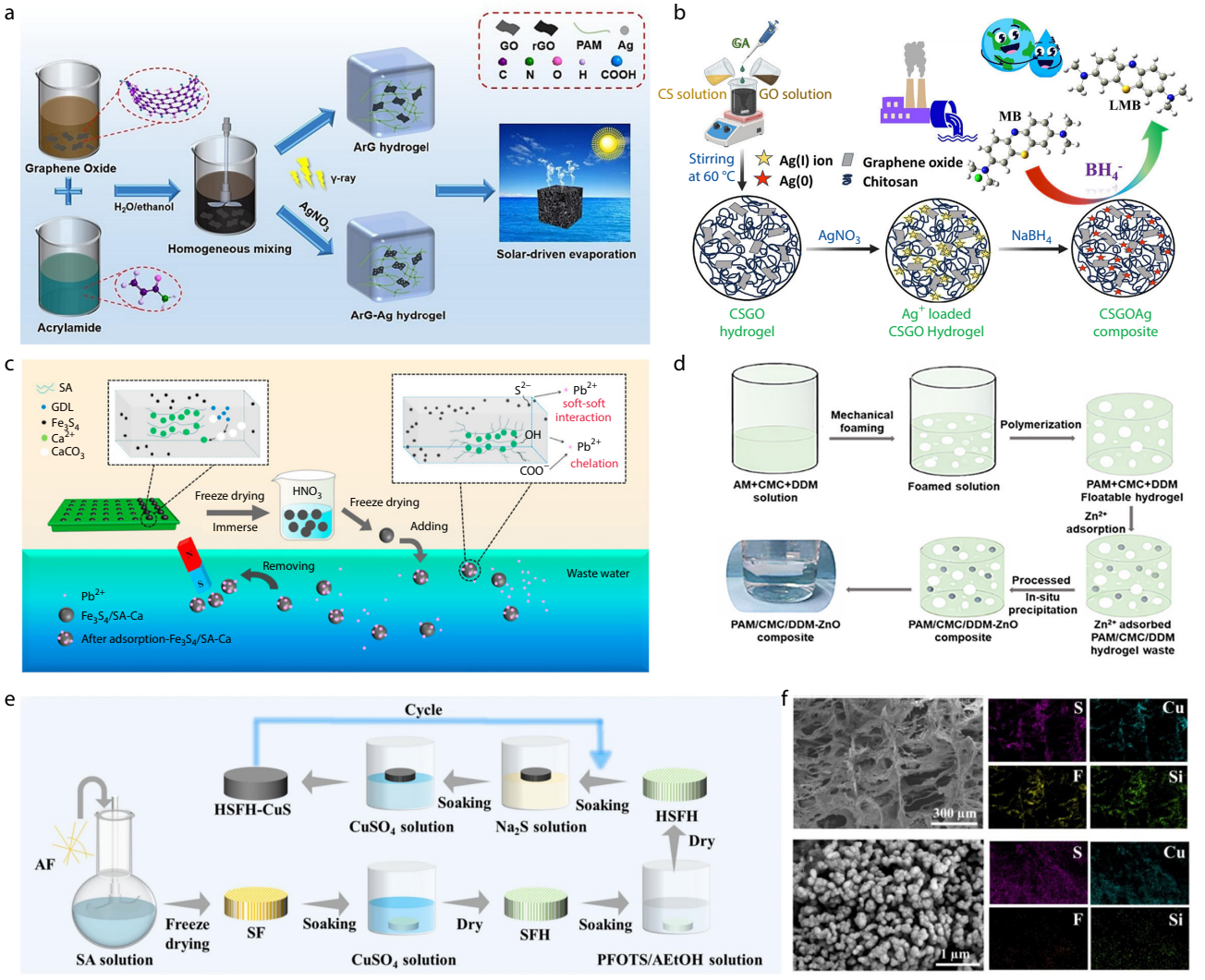

Fig. 5 (a) The irradiation preparation process of ArG and ArG-Ag (Reproduced with permission from Ref. [89]; Copyright (2023), Elsevier); (b) Fabrication of hybrid CSGOAg hydrogel nanocomposites and their use as catalysts in MB degradation (Reproduced with permission from Ref. [90]; Copyright (2025), Elsevier); (c) Preparation of alginate aerogels loaded with sphalerite (Fe_3S_4) (Reproduced with permission from Ref. [91]; Copyright (2022), Elsevier); (d) Schematic diagram of preparation of the floatable PAM/CMC5/DDM hydrogel (Reproduced with permission from Ref. [92]; Copyright (2021), Elsevier); (e) Fabrication process of the HSFH-CuS; (f) SEM image and EDS mapping of the cross-sectional morphology of HSFH and HSFH-CuS. (e, f: reproduced with permission from Ref. [93]; Copyright (2025), Elsevier.)

A representative pathway is to make the hydrogel serve as both a reaction platform and a carrier and to initiate a precipitation reaction directly within its network to generate a catalytically active phase. For example, alginate hydrogels can be enriched with Fe^{+}/Fe^{3+} ions *via* carboxylate coordination, followed by the *in situ* formation of Fe_3S_4 nanoparticles in the presence of S^{2-}, which is then endowed with a self-floating ability by freeze-drying (Fig. 5c).[91] In this process, the hydrogel not only provides an airtight reaction environment but also regulates the homogeneity of the precipitation process and product size distribution through functional group coordination.

Another typical strategy highlights the functional evolution resulting from *in situ* transformation, in which self-floating hydrogels for heavy metal ion adsorption are first constructed and then transformed *in situ* for heavy metal ion reuse. For instance, Zhao and Li used mechanical foaming *in situ* polymerization to prepare low-density self-floating carboxymethyl cellulose/polyacrylamide (PAM/CMC/DDM) hydrogels (Fig. 5d), which were initially used as heavy metal adsorbents. After the adsorption of Zn^{2+}, alkali treatment prompted the *in situ* precipitation of Zn^{2+} in the gel network and its conversion to ZnO nanoparticles, thus realizing the transformation of the material from adsorbent to photocatalyst.[92] This *in situ* precipitation strategy not only enhances the immobilization stability of the active components but also provides an important idea for the multifunctional integration and efficient resource utilization of self-floating hydrogels in water treatment.

In situ polymerization method

The *in situ* polymerization method refers to the direct participation of functional monomers, ligands, or metal complexes in gel polymerization or cross-linking reactions, thus embedding the catalytic centers into the gel network through covalent bond-

ing or stable coordination. Compared with *in situ* reduction and precipitation methods, this strategy is more advantageous in terms of structural stability and interfacial coupling strength.

As shown in Fig. 5(e), Ding *et al.* prepared sodium alginate/aramid fiber (SA/AF) aerogels with oriented pore structures by freeze-drying, followed by ionic cross-linking with SA using Cu^{2+} to form copper alginate hydrogels. In this process, Cu^{2+} acted as both a gel crosslinker and a catalytic precursor, achieving a high degree of synergy between the introduction of active centers and the evolution of the gel structure. The microstructural features of hydrophobically modified HSFH were revealed by SEM imaging (Fig. 5f), showing a typical reticulated gel framework. EDS elemental profiles further indicated that the gel cross-section was enriched with F and Si, confirming the success of the surface modification. In contrast, after *in situ* growth, a large number of CuS nanoparticles with strong Cu and S signals were clearly observed on the HSFH-CuS surface, indicating the successful formation of CuS and its tight interfacial bonding with the hydrogel backbone.[93] The resulting Janus-structured self-floating hydrogel has both a hydrophobic inner layer and a hydrophilic surface layer, which not only achieves stable floating and efficient interfacial heat transfer but also ensures the solid fixation of the CuS catalytic phase through *in situ* polymerization and transformation. This system fully demonstrates the unique advantages of *in situ* polymerization in synergistically regulating structural stability, interfacial function, and catalytic performance.

Post-modification Strategies for Catalyst Loading in Porous Self-floating Gel Matrices

The post-modification loading method refers to the strategy of introducing and immobilizing catalytically active components through chemical or physical interactions after the formation of a gel network. This method is suitable for pre-prepared lightweight porous gels as carriers; subsequently, the abundant active functional groups in the gel network are utilized to anchor the catalytic components *via* covalent bonding or strong adsorption on the pore wall or skeleton surface.[68,94]

The study by Shen *et al.* served as a representative example. In their work, silica colloidal crystal beads (SCCBs) were initially assembled *via* microfluidics as sacrificial templates, and then an acrylamide/acrylic acid (PACA) pre-gel solution was injected into their ordered interstitial space, and PACA hydrogel anti-opalite beads (HIOBs) with three-dimensional periodic structures were obtained by UV-initiated polymerization. After removing the silica template, a regular macroporous array was formed inside the hydrogel, which not only provided a high specific surface area with uniform channels for subsequent catalyst loading but also significantly reduced the density of the material and ensured stable floating. Subsequently, the organic photocatalyst copper phthalocyanine (CuPc) was introduced by the post-impregnation method and firmly anchored to the gel pore wall with the help of Cu-O coordination bonds formed between the Cu^{2+} and —COOH groups in the PACA network (Fig. 6a). Several characterization results confirmed that CuPc was uniformly distributed within the anti-opal structure *via* chemical bonding (Figs. 6b–6g).[95] Thanks to the unique "slow photon effect" of the inverse opal structure and the visible-light responsiveness of CuPc, the composite hydrogel exhibited significantly enhanced light absorption and charge separation efficiency in the photocatalytic degradation of dyes, which fully verified the advantages of the post-catalyst loading strategy in interfacial photocatalytic systems.

Another representative study was conducted by Zhou *et al.* (Fig. 6h). The researchers first constructed a porous gel framework composed of cellulose nanofibers (CNF) and chitosan (CS) by physical cross-linking and obtained a low-density, high-porosity CNF/CS aerogel by freeze-drying. Subsequently, it was immersed in a precursor solution containing Co^{2+}/Fe^{2+} ions with 2-methylimidazole, which induced the *in situ* nucleation and growth of Fe-doped ZIF-67 on the surface of the gel fibers, and the Fe-ZIF-67@CNF/CS composite aerogel was obtained after secondary freeze-drying. As shown in Fig. 6(i), both the pristine and composite aerogels exhibited ultralow densities, which can be held up by dandelions, visually highlighting their lightweight and self-supporting properties. SEM observations further revealed that the Fe-ZIF-67 crystals maintained a well-defined rhombic dodecahedral morphology with an average particle size of approximately 1 μm, whereas the CNF/CS aerogels possessed a three-dimensional interconnected porous network that originated from the template effect of ice crystal growth. Notably, the original pore structure was well preserved in the composite aerogels, whereas the pore walls and fiber surfaces were uniformly decorated with Fe-ZIF-67 crystals, indicating that the MOF phase was effectively integrated without structural collapse.[96] The abundant hydroxyl and amino groups in the CNF/CS matrix promoted the adsorption of metal ions, and the introduction of 2-methylimidazole further strengthened the surface metal coordination, which achieved *in situ* nucleation, uniform growth, and stable cementation of Fe-ZIF-67 crystals, and effectively avoided the *in situ* nucleation of the crystals. Stabilized solid loading was achieved to avoid free aggregation of crystals in the solution. The post-modified loading method realizes functional synergy between the porous carrier and catalytically active components through a step-by-step construction strategy, which lays a solid foundation for the preparation of high-performance composites.

As shown in Table 1, a direct comparison of the three principal construction strategies highlights their unique features, thereby providing a clear framework for selecting an appropriate approach based on specific application demands. The precursor blending method, which relies on physical entrapment, stands out for its simplicity and minimal procedural complexity, rendering it well-suited for rapid prototyping and cost-sensitive scenarios. However, this comes at the expense of a relatively uneven catalyst distribution and a limited binding strength. By contrast, *in situ* synthesis promotes more homogeneous catalyst dispersion through physical adsorption during gel formation, striking a moderate balance between binding strength and process intricacy. When applications require maximal durability and interfacial stability, the post-modification strategy can ensure both superior binding and excellent dispersion by establishing covalent linkages between the catalyst and hydrogel matrix, albeit with a more elaborate synthesis procedure. Taken together, this comparative evaluation demonstrates that the optimal strategy depends critically on priorities such as process efficiency, catalyst utilization, and long-term operational stability, thus offering a more nuanced delineation of the advantages and limitations of each method.

https://doi.org/10.1007/s10118-026-3578-9

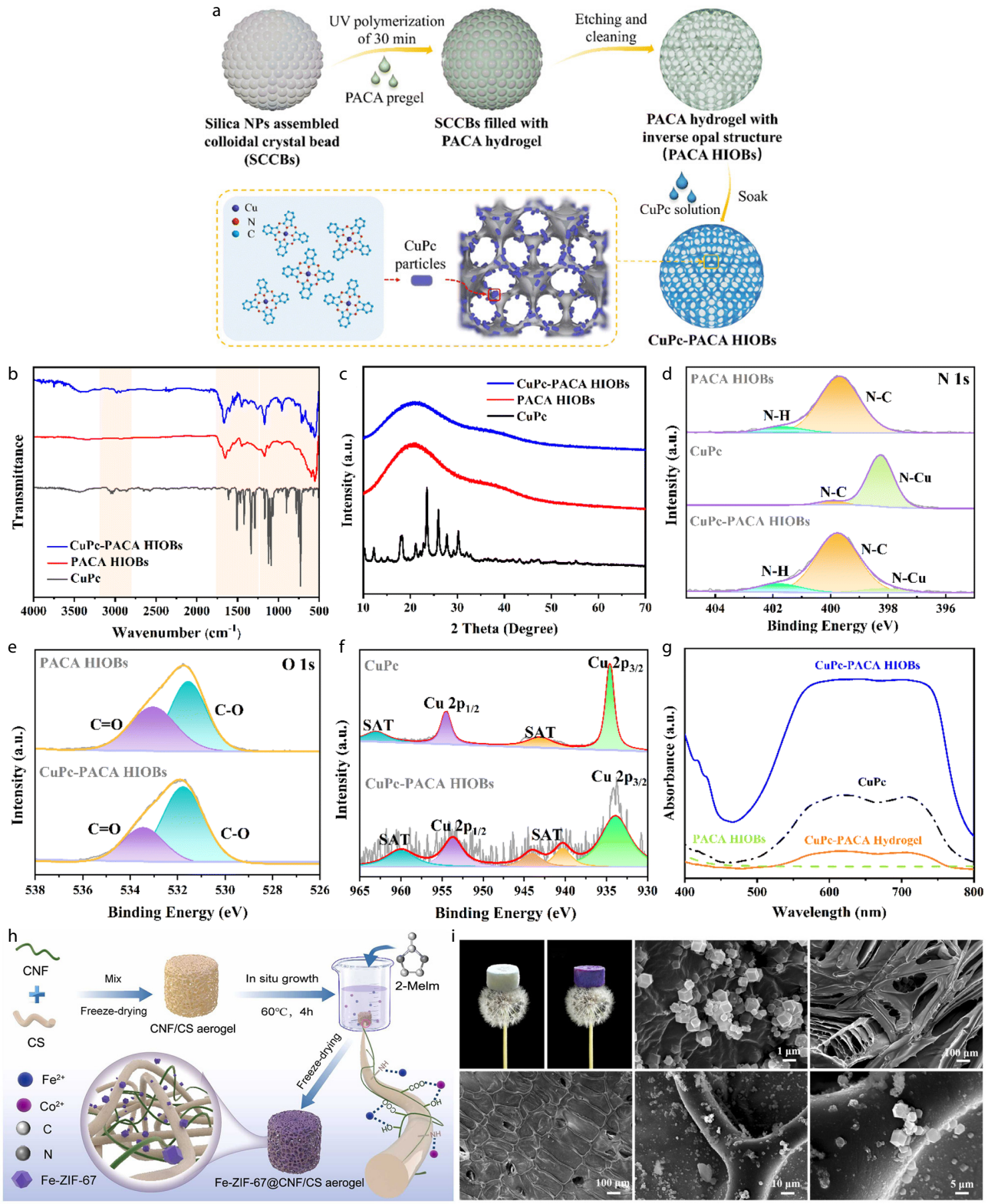

Fig. 6 (a) Schematic diagram of the preparation of CuPc-PACA HIOBs; (b) FTIR spectra, (c) XRD, (d–f) HRXPS spectra, and (g) UV-Vis DRS spectra of the samples including CuPc, CuPc-PACA hydrogels, PACA HIOBs, and CuPc-PACA HIOBs. (a–g: reproduced with permission from Ref. [95]; Copyright (2023), Royal Society of Chemistry.) (h) Schematic flow diagram of the synthesis of Fe-ZIF-67@CNF/CS; (i) Digital photos of CNF/CS aerogel and Fe-ZIF-67@CNF/CS aerogel; SEM images of Fe-ZIF-67, CNF/CS aerogel and Fe-ZIF-67@CNF/CS aerogel. (h, i: reproduced with permission from Ref. [96]; Copyright (2025), Elsevier.)

https://doi.org/10.1007/s10118-026-3578-9

Table 1 Comparison of representative construction strategies for hydrogel-based self-floating catalytic materials.

Construction strategy	Gel/catalyst	Core interaction	Floating strategy	Advantages	Limitations	Ref.
Precursor blending	PVA/CuO;ATO	Physical entrapment; Hydrogen bond	Sacrificial template	Facile process; Broad applicability	Poor stability; Non-uniform distribution; Potential interference with gelation	[82]
	CMC;PVA/Lac@HOF-101	Physical entrapment; Coordination bond; Hydrogen bond	Freeze drying			[84]
	PVA;SA/MXene	Physical entrapment; Hydrogen bond	Directional freeze-casting			[85]
	SA;BC/Fe-ZnO	Physical entrapment; Coordination bond; Hydrogen bond	Freeze drying; Hydrophobic modification			[86]
In situ synthesis	PAM;rGo/Ag	Physical confinement; Coordination bond; Hydrogen bond	Oven drying	High dispersion; Strong stability; Controllable loading	Multi-step process; Optimization of conditions needed	[89]
	CS;GO/Ag	Physical confinement; Coordination bond; Electrostatic interaction	Freeze drying			[90]
	SA/Fe_3S_4	Physical confinement; Coordination bond;	Freeze drying			[91]
	PAM;CMC;DDM/ZnO	Physical confinement; Coordination bond; Electrostatic interaction	Mechanical foaming			[92]
	SA;AF/CuS	Physical confinement; Coordination bond; Electrostatic interaction	Freeze drying			[93]
Post-modification	PACA/CuPc	Coordination bond; Covalent Bond	Sacrificial template	Strong anchoring & stability; High flexibility	Most complex process	[95]
	CNF;CS/Fe-ZIF-67	Coordination bond; Covalent Bond; Electrostatic interaction	Freeze drying			[96]

Summary of Strategies for Self-floating Gel Structures

Combining the three strategies of precursor mixing, *in situ* synthesis, and post-modified loading, it can be seen that the construction of floating gel catalytic materials relies not only on the introduction method of catalysts, but more critically on the rational design of lightweight self-floating gel structures. In existing studies, freeze-drying, sacrificial templates, and physical foaming have been widely used to construct low-density porous gel skeletons, which constitute the core engineering tools for the stable floating of materials at the water-gas interface.

In gel-based self-floating materials, lightweight structures are usually realized using templating methods, foaming, and compositional adjustment strategies. Among them, the template method is the dominant technology owing to its excellent structural controllability, covering the ice template, emulsion template, and sacrificial template methods. Ice templating (especially directional freeze casting) utilizes ice crystal nucleation and growth to form interconnected macropores or highly oriented channels in the gel matrix (Fig. 7a), which not only significantly reduces the density of the material but also contributes to the efficient transport of water and reactants.[97] As shown in Fig. 7(b), the emulsion template method introduces a stably dispersed liquid phase as a soft template during gel formation, which is "locked" into the gel network by polymerization or cross-linking.[98] Sacrificial templating methods, such as the use of salt particles (Fig. 7c) can produce porous frameworks with regular morphology and tunable structure;[99] similarly, polymer microspheres or SiO_2 colloidal crystals are often used for pore creation as removable phases.[96]

The foaming method introduces gases directly into the system through physical (mechanical stirring, Fig. 7d)[100] or chemical (CO_2 release from blowing agents during gelation, Fig. 7e)[101] to form pore structures. In addition, 3D printing technology can be used to directly construct gel structures with preset pore channels and density distributions at the macroscopic scale by precisely controlling the printing path and filling pattern, achieving the integration of lightweighting and functional integration (Fig. 7f).[102]

Beyond structural engineering, compositional regulation also plays a critical role in achieving stable self-floating behavior. The introduction of hydrophobic components (Fig. 7g) or lightweight fillers (Fig. 7h) can effectively reduce the apparent density and wettability of the materials to stabilize them at the water-gas interface, while maintaining sufficient mechanical strength and enhancing functional properties.[103,104]

APPLICATIONS

Hydrogel-based self-floating catalytic materials have been widely applied in various environmental and energy-related fields owing to their tunable three-dimensional polymer networks, hierarchical porous structures, and stable localization at the gas-liquid interface.[76–79] Numerous studies have confirmed that such interfacial configurations can improve light-energy utilization, effectively alleviate mass-transfer limitations, and significantly enhance the operational stability of catalytic systems in complex multiphase reaction environments.[105–107] To illustrate the practical manifestation of these advantages, the following section selects some representative applications to reveal the intrinsic correlation between the material structure design and construction strategies and the final catalytic performance.

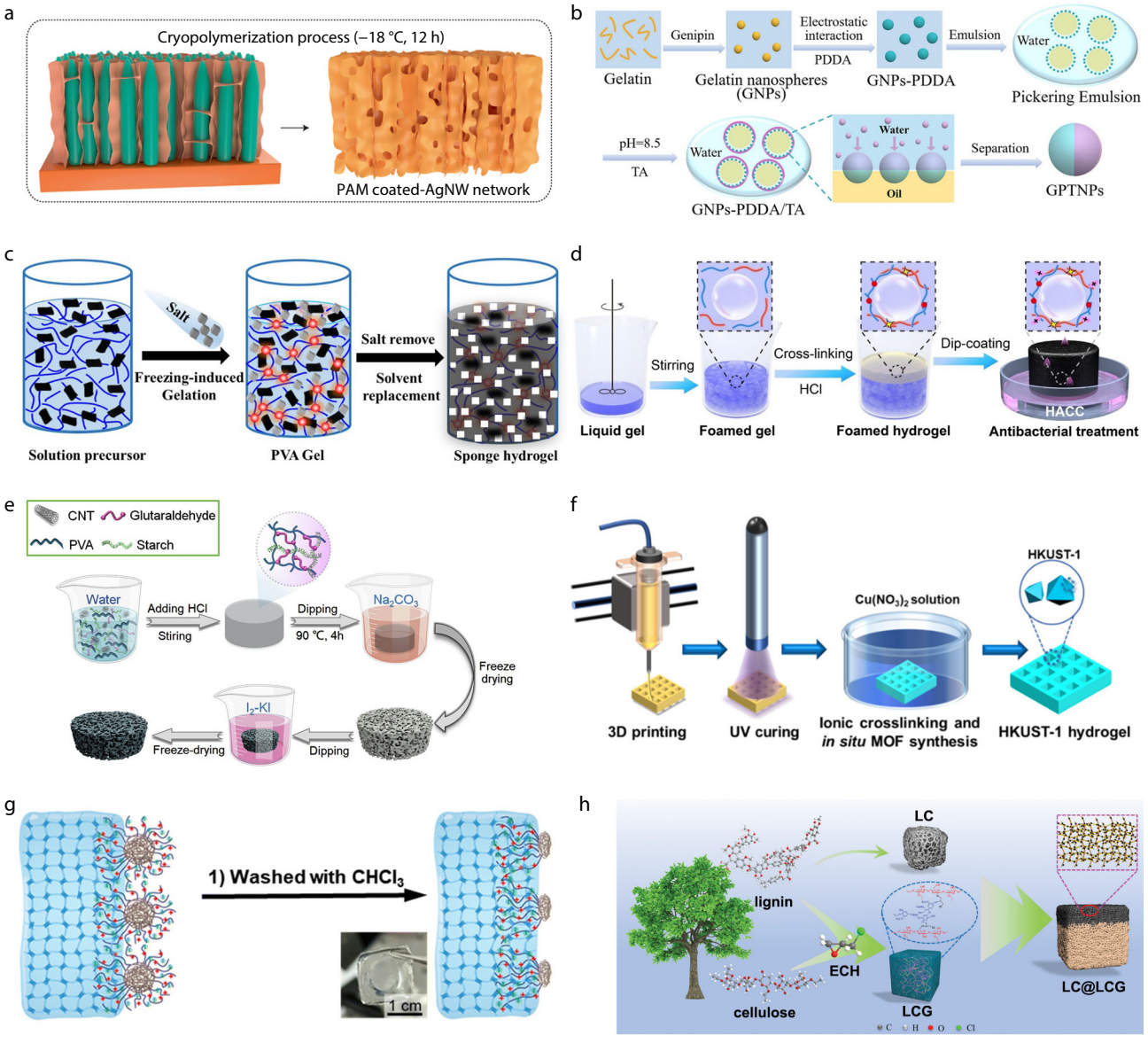

Fig. 7 (a) Schematic illustration of the fabrication of the CCAP hydrogel by the combined directional freezing assembly (Reproduced with permission from Ref. [97]; Copyright (2022), Springer Nature); (b) Flow chart of the preparation of GPTNPs (Reproduced with permission from Ref. [98]; Copyright (2023), Elsevier); (c) Schematic diagram of the process of fabricating sponge like hydrogel through a facile and scalable salt template method (Reproduced with permission from Ref. [99]; Copyright (2022), Elsevier); (d) A flow chart of fabrication of the SA/PVA/HACC hydrogel foam (Reproduced with permission from Ref. [100]; Copyright (2022), Elsevier); (e) Scheme of preparing multifunctional PSIGx hybrid hydrogel evaporator (Reproduced with permission from Ref. [101]; Copyright (2022), Elsevier); (f) Schematic showing the three critical steps in the 3D printing process including printing, UV curing, and ionic cross-linking (Reproduced with permission from Ref. [102]; Copyright (2020), American Chemical Society); (g) Schematic illustration of electric-field grafting of charged micelles onto the hydrogel (Reproduced with permission from Ref. [103]; Copyright (2024), Royal Society of Chemistry); (h) Synthesis schematic of lignocellulosic biomass-based double-layered porous hydrogel LC@LCG for ISSG (Reproduced with permission from Ref. [104]; Copyright (2022), John Wiley and Sons).

Catalytic Degradation of Organic Pollutants

Hydrogel-based self-floating catalytic materials have become efficient AOP platforms for the degradation of organic pollutants due to their interfacial advantages. The continuous three-dimensional network not only actively traps and enriches pollutant molecules but also provides a domain-limited environment for the loading of catalytically active components.[46,57,58,74,75] In recent years, a large number of studies have shown that such materials exhibit significant advantages in the removal of typical pollutants such as dyes, phenolic compounds, antibiotics, and micro/nano plastics.

Dyes, which are typical recalcitrant organic pollutants in industrial wastewater, are difficult to decompose under natural conditions because of their stable aromatic conjugated structure and strong photostability.[108] Hydrogel-based self-floating catalytic materials exhibit significant advantages in optimizing the interfacial environment. Amornpitoksuk *et al.* successfully constructed a floating hydrogel system with high

porosity and excellent structural stability by modulating the cross-linking density of the PAM gels (Fig. 8a). The system significantly enhanced the local enrichment efficiency of dye molecules at the gas-liquid interface, which dramatically accelerated the interfacial catalytic degradation reaction process (Fig. 8b) and maintained low metal ion dissolution during the operation (Fig. 8c).[109] The incorporation of active components such as TiO_2, CuO, Fe_3O_4, or Bi-based composites enabled the continuous generation of ROS under light or peroxide activation, improving light utilization and alleviating mass transfer limitations, thereby achieving efficient pollutant removal.

Antibiotics are of great concern because of their wide distribution in the aquatic environment, high chemical stability, and potential ecological risks, while phenolic compounds are another major challenge in the field of water treatment because of their high toxicity and environmental persistence.[110] Such pollutants place higher demands on the efficiency and long-term stability of the treatment technologies. Catalytic systems based on self-floating gels exhibit excellent pollutant removal capabilities by effectively combining an adsorption enrichment function with advanced oxidation processes. Taking the $CuBi_2O_4$/rGH composite system as an example, the graphene hydrogel achieved rapid adsorption and

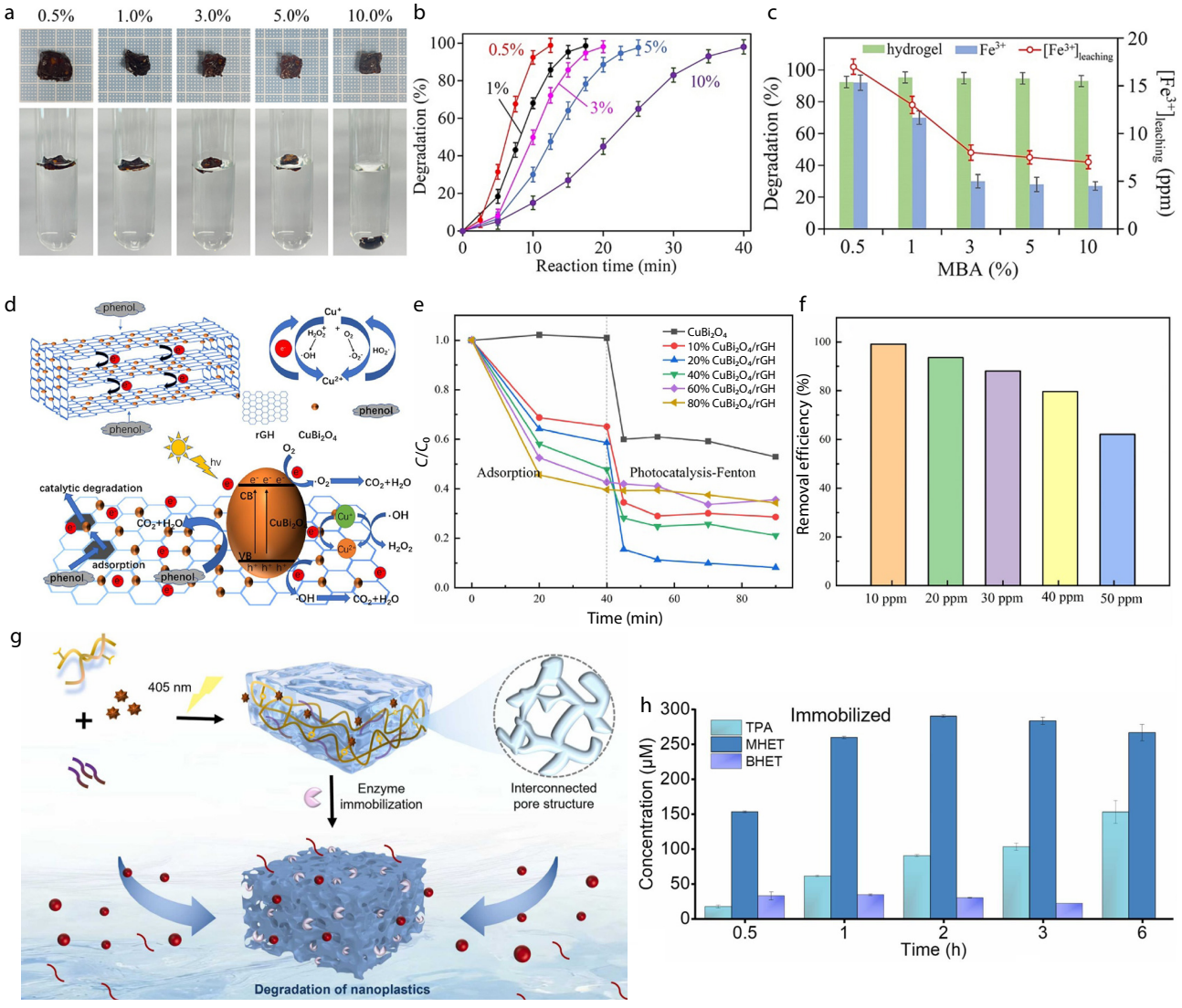

Fig. 8 (a) Photographs of the Fe-PAM hydrogels floating on the surface of the water; (b) RhB degradation by Fe-PAM hydrogels at different MBA contents with H_2O_2; (c) RhB degradation by Fe-PAM hydrogels at different MBA contents (green bar) and Fe^{3+} ions at equal concentrations to Fe^{3+} leaching (blue bar) and concentrations of Fe^{3+} leaching from Fe-PAM hydrogels at different MBA contents (red line); (a–c: reproduced with permission from Ref. [109]; Copyright (2024), Elsevier.) (d) Mechanism diagram of $CuBi_2O_4$/rGH adsorption and *in situ* photocatalytic Fenton catalytic degradation of phenol. Adsorption-catalytic degradation performance of the $CuBi_2O_4$/rGH composite for phenol (e) different rGH contents (catalyst=20 mg, C_0=20 mg/L, pH=7, [H_2O_2]=10 mmol/L) and (f) different phenol concentrations (catalyst=20 mg, pH=7, [H_2O_2]=10 mmol/L); (d–f: reproduced with permission from Ref. [111]; Copyright (2023), Elsevier.) (g) Illustration of the preparation of enzyme-loaded porous hydrogels; (h) The concentration change of different products during a 6-hour degradation process conducted at 50 °C; (g, h: reproduced with permission from Ref. [112]; Copyright (2025), Elsevier.)

enrichment of phenolic pollutants through π-π interactions, whereas the loaded $CuBi_2O_4$ could synergistically activate H_2O_2 under light to continuously generate strong oxidizing radicals, mainly ·OH (Fig. 8d). The confined gel matrix prevents nanoparticle agglomeration and maintains full exposure of active sites, and the floating structure further enhances interfacial mass transfer and light utilization. This synergy allows rapid pollutant adsorption and deep mineralization *via* photocatalytic-Fenton coupling, maintaining high removal efficiency even at elevated initial concentrations (Figs. 8e and 8f).[111]

Micro/nano plastics, as an emerging and particularly challenging class of pollutants, further expand the scope of applications of hydrogel-based self-floating catalytic materials.[94] Owing to their small size, hidden distribution, and high chemical stability, it is difficult to effectively remove micro/nano plastics using conventional physical or chemical methods. Although increasing attention has been devoted to catalytic and enzymatic degradation strategies, practical implementation remains challenging because of the intrinsically slow degradation kinetics, limited long-term stability of catalysts or enzymes, and inhibitory effects of complex water matrices containing natural organic matter, inorganic ions, and suspended solids.

Zhang *et al.* developed a low-density porous gel fabricated by photocrosslinking and freeze-drying that could effectively capture PET nano plastics through its internal pores and simultaneously stably immobilize hydrolytic enzymes within the gel framework (Fig. 8g). Attributed to the confinement effect of the gel matrix, the contact frequency between the enzyme and the substrate was significantly increased, which accelerated PET degradation and resulted in the rapid formation of degradation products, such as terephthalic acid (TPA), mono(2-hydroxyethyl) terephthalate (MHET), and bis(2-hydroxyethyl) terephthalate (BHET) (Fig. 8h). The thermal stability, solvent resistance, and recoverability of the immobilized enzyme were significantly improved compared with those of the free enzyme system.[112] More broadly, hydrogel-based self-floating catalytic systems offer unique structural and interfacial advantages for addressing these challenges. The three-dimensional polymer network provides a confined microenvironment that stabilizes catalytic or enzymatic species and inhibits aggregation or leaching, while the floating structure ensures continuous access to light and oxygen at the air-water interface. Simultaneously, the hydrogel matrix promotes localized enrichment of micro/nano plastics, oxidants, and reaction intermediates, thus partially offsetting the slow intrinsic reaction rates under dilute conditions. Nevertheless, the application of self-floating hydrogels for micro/nano plastics degradation is still at an early stage, with most studies focusing on single-polymer types and laboratory-scale systems. Therefore, further systematic studies are needed to investigate their performance under complex real-world water quality conditions and during long-term operations.

Solar-driven Energy and Resource Conversion

Hydrogel-based self-floating catalytic materials show significant potential for solar-powered energy conversion and chemical synthesis, covering a variety of applications such as hydrogen preparation, chemical fuel synthesis, and high-value oxidant generation.[29] In practical reaction systems, achieving efficient light energy capture, fast carrier separation, and smooth multiphase substance transport remain the core challenges in enhancing photocatalytic efficiency. By virtue of its lightweight and porous nature, the self-floating gel can stably stay at the gas-liquid interface and form a unique three-phase reaction zone, minimizing the absorption and scattering loss of light by the water in the bulk phase and significantly shortening the diffusion distance from the reactants to the active sites, thus realizing efficient energy conversion.[46,74]

In the photocatalytic hydrogen production process, these materials provide an ideal interfacial platform for water decomposition. The three-dimensional network can firmly load highly dispersed photocatalysts, effectively preventing particle agglomeration and sedimentation, whereas the through-pore structure and hydrophilic skeleton can enrich water molecules at the interface to ensure a continuous supply of reactants.[14,17] Taking a Pt/Ti oxide photocatalyst embedded in a durable elastomer-hydrogel composite system (HPU-PPG) as an example, the material can float stably on the water surface, realizing highly efficient light transmission, smooth hydrogen escape, and long-term stable operation of the catalyst (Fig. 9a). The floating ability of the material was further enhanced by introducing a hydrophobic silica aerogel layer, which prevented the material from being submerged in water. Benefiting from the above structural and interfacial properties, the system maintained a stable hydrogen precipitation rate of approximately 150 mmol/(h·m^2) for seven consecutive days (Fig. 9b), indicating that the hydrogel-based self-floating catalytic materials are expected to be a low-cost, high-efficiency, and high-stability platform for photocatalytic hydrogen production.[113]

In traditional aqueous photocatalytic systems, the mass transfer process of gaseous reactants often becomes a key bottleneck for efficiency enhancement due to their limited solubility and long diffusion path. In contrast, hydrogel-based self-floating catalytic materials significantly accelerate the reaction rate and improve the product selectivity by stabilizing at the gas-liquid interface, which enables the gas molecules to directly contact and enrich the catalytically active sites. A typical study is the hydrophilic floating hydrogel membrane system (Fe(III)@CAN) constructed by He *et al.*, which successfully establishes a stable three-phase interface (Fig. 9c). Methane molecules rapidly diffuse and undergo initial activation on the gel surface, while the hydrophilic channels running through the gel interior promote *in situ* generation and local accumulation of hydrogen peroxide. Under light, the system initiated the photo-Fenton reaction under mild conditions to achieve the highly selective oxidation of methane to ethanol in an atmospheric pressure environment. The domain-limited microenvironment provided by the gel can precisely regulate the concentration of free radicals and effectively inhibit over-oxidation and side reactions that are prone to occur in the conventional system, thus significantly enhancing the selectivity and efficiency of the target products (Figs. 9d and 9e).[114] The hydrogel-based self-floating catalytic system not only opens up a new way for the high-value conversion of methane, but also provides a design idea that

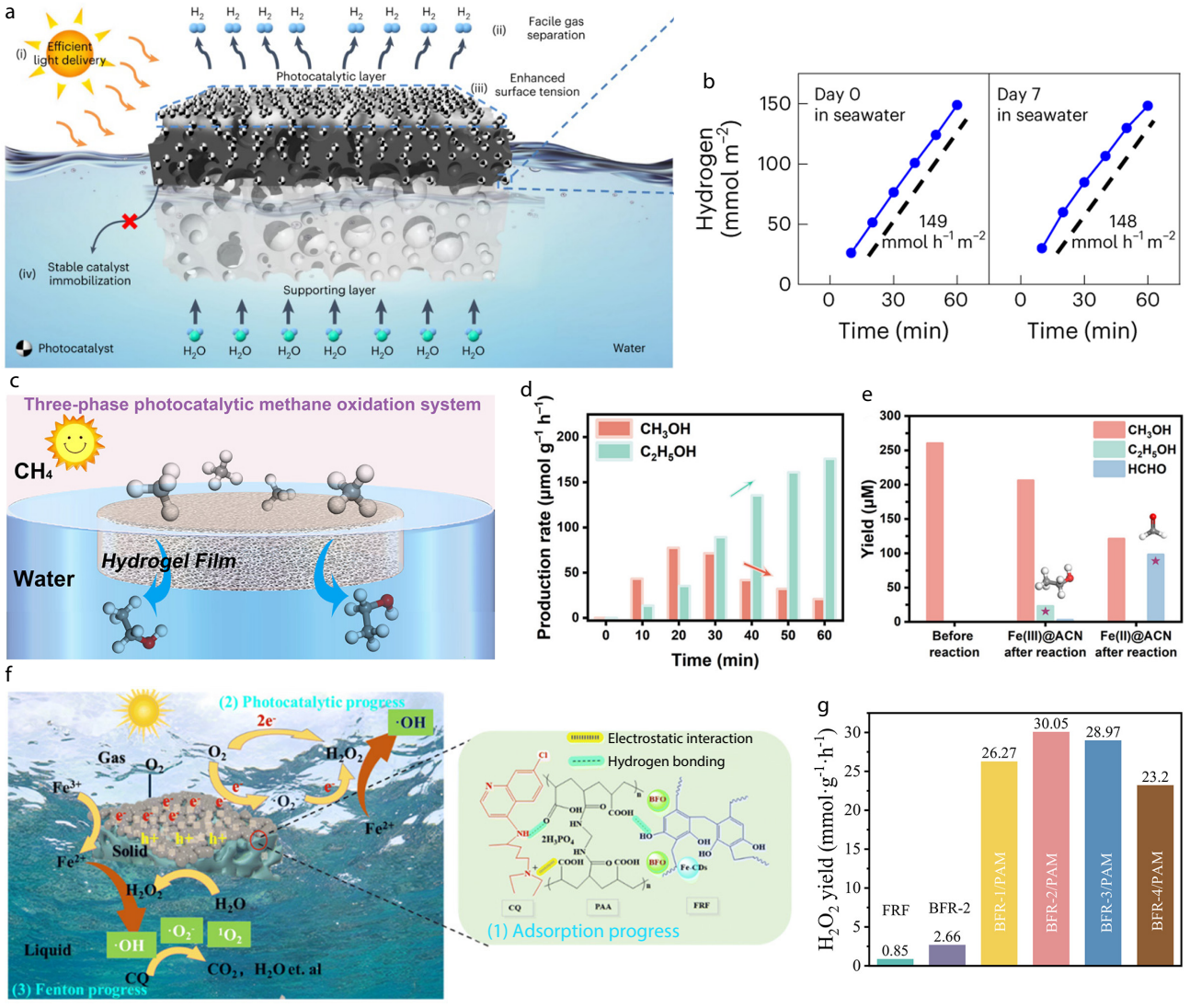

Fig. 9 (a) Schematic of the nanocomposites and their advantages for photocatalytic HER; (b) Longterm time course of H_2 production in seawater; (a, b: reproduced with permission from Ref. [113]; Copyright (2023), Springer Nature.) (c) Hydrophilic floating hydrogel for photocatalytic methane oxidation at the three-phase interface; (d) Reaction time of CH_3OH and C_2H_5OH evolution in Fe(III)@ACN system; (e) CH_3OH conversion catalyzed by Fe(III)@ACN and Fe(II)@ACN with 0.26 mmol/L CH_3OH in H_2O under Ar atmosphere (reaction time: 0.5 h); (c–e: reproduced with permission from Ref. [114]; Copyright (2024), American Chemical Society.) (f) Possible synergistic degradation mechanism of BFR/PAA in photo-self-Fenton systems; (g) The H_2O_2 yield of samples after 30 min with Xe lamp irradiation ($\lambda > 420$ nm). (f, g: reproduced with permission from Ref. [115]; Copyright (2025), The Royal Society of Chemistry.)

can be used for gas-liquid interface reaction processes, such as CO_2 photocatalytic reduction and O_2 activation.

In addition, a hydrogel-based self-floating catalytic system is crucial for the *in situ* generation of H_2O_2 and its coupling with advanced oxidation processes. H_2O_2, as a green oxidant and energy carrier, can be efficiently synthesized *via* the key photocatalytic pathway of the two-electron oxygen reduction reaction. When the photocatalyst is cemented in a self-leafing gel, it can effectively catalyze the oxygen reduction reaction at the gas-liquid interface to achieve continuous generation of H_2O_2. The porous network further facilitates oxygen diffusion and electron transfer to maintain a highly localized concentration of H_2O_2 in the limited microenvironment. For example, in the BFR/PAA system, the heterojunction structure enhanced the photogenerated electron transfer efficiency, enabling the H_2O_2 generation rate of the BFR-2/PAA composite catalyst to reach 30.05 mmol/(g·h) in light (Figs. 9f and 9g). Interestingly, the generated H_2O_2 can be instantly utilized *in situ*, and the metal active sites in the gel skeleton synergistically interact with it to trigger the photo-Fenton reaction, which continuously generates highly reactive ·OH. These radicals can efficiently degrade antibiotics and pharmaceutical pollutants in a gel-enclosed environment for rapid mineralization.[115] Hydrogel-based self-floating catalytic materials enhance mass transfer and local enrichment effects, while enabling efficient *in situ* H_2O_2 synthesis and immediate utilization, thereby offering an effective and stable approach for rapid pollutant degradation and solar-driven chemical transformations.

Synergistic Catalysis for Interfacial Evaporation

Hydrogel-based self-floating catalytic materials exhibit multiple synergistic functions in solar-driven desalination, combining interfacial photothermal evaporation, photocatalytic reactions, and coupled energy utilization to realize the integrated operation of pollutant removal and high-efficiency freshwater production.[28,45] The porous framework enables rapid capillary transport of water through interconnected hydrophilic channels to ensure sufficient water supply to the evaporation interface, while the inherently low thermal conductivity of the hydrogel helps concentrate the absorbed solar energy on the surface, thus enhancing the evaporation flux and light-vapor conversion efficiency. The self-floating structure minimizes the heat loss of water in the bulk phase, which not only improves the energy efficiency but also guarantees the stability of the system operation.[7] The continuous high temperature at the interface also inhibits local salt analysis and crystallization, effectively preventing pore clogging and maintaining a stable and continuous freshwater output, even when dealing with high-salinity seawater or brine.[104]

Li *et al.* fabricated a fully bio-based porous hydrogel evaporator with a core-shell architecture using SA as the matrix and pulp fibers (PF) as reinforcement. Subsequent *in situ* generation of CuS nanoparticles on the surface layer of SA by immersion in a Na_2S solution dramatically enhanced the photothermal conversion capability. With the surface-constructed trapezoidal microstructure (Fig. 10a) and Marangoni effect-guided interfacial salt migration (Fig. 10b), the evaporator exhibited excellent salt resistance during long-term operation, maintaining a stable evaporation rate of 2.42 kg/(m²·h).[116]

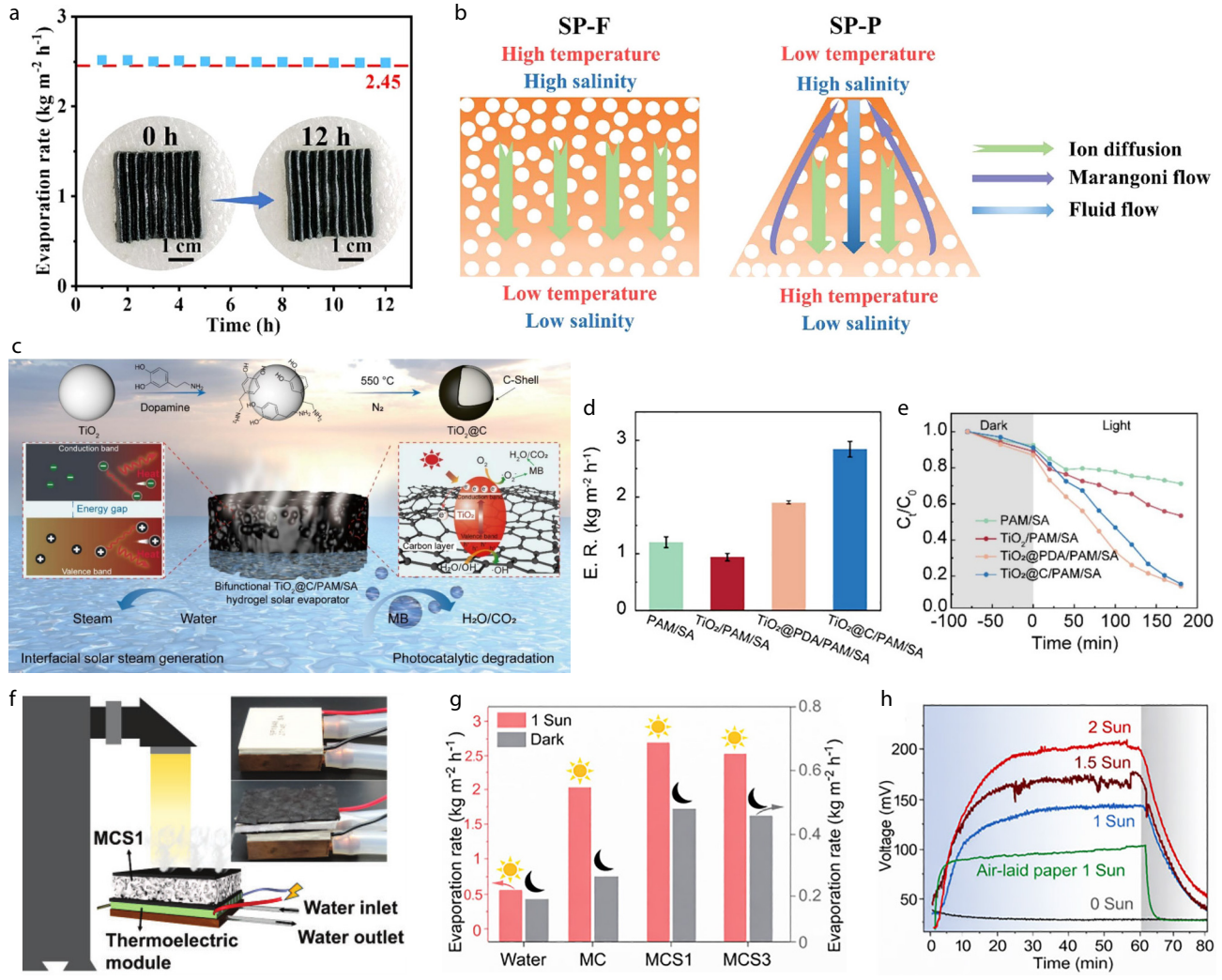

Fig. 10 (a) Evaporation rate of SP-P in 10 wt% saltwater for 12 h under 1.0 sun, with insets showing photographs of SP-P before and after evaporation; (b) Schematic diagram of the Marangoni effect induced on the surface of SP-P; (a, b: reproduced with permission from Ref. [116]; Copyright (2025), Elsevier.) (c) Schematic diagram of synergistic photothermal and photocatalytic degradation mechanism of TiO_2@C/PAM/SA hydrogels; (d) Evaporation rates of the PAM/SA, TiO_2/PAM/SA, TiO_2@PDA/PAM/SA, and TiO_2@C/PAM/SA hydrogel under one sun irradiation during the evaporation process; (e) Photodegradation performances of bifunctional TiO_2@C/PAM/SA hydrogel solar evaporator; (c–e: reproduced with permission from Ref. [117]; Copyright (2025), Elsevier.) (f) Scheme of the setup used for steam and thermoelectricity cogeneration; (g) Evaporation rates of various evaporators under solar light on or off mod; (h) V_{OC} of the assembled device under light on and off modes (lower surface temperature: 20 °C). (f–h: reproduced with permission from Ref. [118]; Copyright (2023), John Wiley and Sons.)

The hydrogel-based self-floating catalytic system achieves synergy between desalination and pollutant degradation by coupling the photothermal evaporation and photocatalytic processes. For example, in the TiO_2@C/PAM/SA floating gel catalytic system, the incorporated carbon layer significantly enhances visible light absorption while facilitating the effective separation and migration of photogenerated carriers in TiO_2, thereby achieving efficient pollutant degradation coupled with interfacial evaporation (Fig. 10c). The experimental results showed that under 1 solar irradiation, the hydrogel exhibited a linear mass loss within 60 min, corresponding to an evaporation rate of 2.97 kg/(m^2·h) (Fig. 10d), and the degradation efficiency of methylene blue (MB) reached 84.37% after 180 min of sustained light exposure (Fig. 10e), demonstrating excellent pollutant removal performance.[117] This synergistic model, which significantly enhances the overall efficiency of the advanced oxidation process, provides a promising technological pathway for the desalination of seawater containing organic pollutants.

Furthermore, self-floating gels can be integrated with photoelectrochemical processes for integrated energy utilization. By constructing conductive networks or semiconductor heterojunctions in the matrix, it is possible to synergize photothermal evaporation with photovoltaic conversion. Such design ideas have been validated in a biomimetic all-weather solar evaporator: inspired by the temperature control mechanism of antifreeze proteins in beetles, the researchers developed a "sandwich" structured evaporator (MCSX), with MnO_2-modified cotton fabric (MC) on the top and the bottom layers for high efficiency of photo-thermal absorption and conversion, and an intermediate layer of phase change microcapsule/poly(vinyl alcohol) (PCL/PVA) hydrogel was used for thermal energy storage and regulation (Fig. 10f). Under light conditions, the evaporation rate reaches 2.67 kg/(m^2·h); in the absence of light, the latent heat released from the PCL layer maintains an evaporation rate of 0.43 kg/(m^2·h) (Fig. 10g). After integrating the thermoelectric (TE) module, the system can provide a stable power output of about 0.42 W/m^2, and the power generation can continue for about 30 min after the light stops (Fig. 10h), which fully demonstrates the superiority of the multi-modal coupling of photo-thermal-energy storage-power generation.[118]

CONCLUSIONS AND FUTURE PERSPECTIVES

Hydrogel-based self-floating catalytic materials are an emerging and fast-growing innovation platform in the field of solar-driven chemistry, especially in the past five years, and have provided a unique bridge between fundamental catalytic research and practical environmental and energy-related applications. By combining lightweight porous structures with stable interfacial localization, these systems effectively address the long-standing limitations of conventional dispersed catalysts, including their low mass transfer efficiency, active site aggregation, and suboptimal solar energy utilization. This review systematically summarizes three representative construction strategies (precursor blending, *in situ* synthesis, and post-modification) and highlights their roles in enabling orderly integration of photocatalysis, Fenton-type reactions, and photothermal conversion within self-floating hydrogel matrices.

A distinctive feature of these materials is the formation of gas-liquid-solid interfaces that combine pollutant adsorption and enrichment with interfacial catalytic reactions, resulting in synergistic performance enhancement. This interfacial reaction mode has been shown to significantly facilitates advanced oxidative degradation and solar-driven energy conversion. As a result, hydrogel-based self-floating catalytic systems have been successfully explored for a wide range of applications, including the removal of recalcitrant pollutants, solar-driven hydrogen production, value-added chemical synthesis, and multifunctional solar-powered seawater desalination.

Despite these advances, several critical scientific and technological bottlenecks continue to limit large-scale and long-term applications. From a material design perspective, maintaining structural integrity, catalytic accessibility, and chemical stability under harsh or fluctuating environmental conditions remains a challenge, especially for highly porous and lightweight gel structures. At the interfacial reaction level, there is still a lack of quantitative understanding of the mass transfer, reactant generation, and kinetic processes within closed hydrogel networks and at floating interfaces, which hampers rational structural performance optimization. From an engineering and implementation perspective, systematic validation beyond laboratory-scale demonstrations is required to achieve scalable fabrication, reproducibility, fouling resistance, and sustained performance in complex, real-world water matrices.

Addressing these challenges requires coordinated progress in multiple directions. Future work should focus on the development of stimulus-responsive and adaptive hydrogel systems with tunable catalytic behavior, deeper integration of photocatalysis, Fenton chemistry, photothermal conversion, and adsorption in a unified material platform, and a combination of *in situ* characterization techniques and multiscale simulations to elucidate the relationship between the material structure, active site configuration, and interfacial reaction kinetics. Equally important is the evaluation of the practical performance through pilot-scale testing in realistic aqueous environments. In parallel, the use of biodegradable or waste-derived raw materials and recycling-oriented design strategies are essential to improve the overall sustainability of these systems.

In conclusion, by precisely tuning the microstructural and interfacial properties, hydrogel self-floating catalysts are expected to evolve from passive catalyst carriers to programmable and multifunctional interfacial chemical reactors, thereby opening new avenues for sustainable water treatment and solar energy conversion technologies.

BIOGRAPHY

Wen-Wei Lei is an Associate Professor at Yanshan University. He earned his Ph.D. in July 2019 from Beihang University, under the supervision of Academician Lei Jiang. Following his doctorate, he conducted postdoctoral research at the International Research Center for Photocatalysis, Tokyo University of Science, Japan. In March 2021, he joined the School of Environmental and Chemical Engineering at Yanshan University as Distinguished Talent (Category A). His primary research focuses on

https://doi.org/10.1007/s10118-026-3578-9

bio-inspired smart interfacial materials and polymer gel composites.

Conflict of Interests

The authors declare no interest conflict.

ACKNOWLEDGMENTS

This work was financially supported by the Cultivation Project for Basic Research and Innovation of Yanshan University (No. 2022LGQN006).

REFERENCES

1 Sun, X. D.; Jiang, S. Y.; Huang, H. W.; Li, H.; Jia, B. H.; Ma, T. Y. Solar energy catalysis. *Angew. Chem. Int. Ed.* **2022**, *61*, e202204880.
2 He, J.; Janáky, C. Recent advances in solar-driven carbon dioxide conversion: Expectations versus reality. *ACS Energy Lett.* **2020**, *5*, 1996–2014.
3 Huang, Y. Y.; Shen, M. H.; Yan, H. J.; He, Y. G.; Xu, J. Q.; Zhu, F.; Yang, X.; Ye, Y. X.; Ouyang, G. F. Achieving a solar-to-chemical efficiency of 3.6% in ambient conditions by inhibiting interlayer charges transport. *Nat. Commun.* **2024**, *15*, 5406.
4 Mao, K.; Zhang, Y. X.; Tan, S. C. Functionalizing solar-driven steam generation towards water and energy sustainability. *Nat. Water* **2025**, *3*, 144–156.
5 Wang, A. W.; Du, M.; Ni, J. X.; Liu, D. Q.; Pan, Y. H.; Liang, X. Y.; Liu, D. M.; Ma, J.; Wang, J.; Wang, W. Enhanced and synergistic catalytic activation by photoexcitation driven S-scheme heterojunction hydrogel interface electric field. *Nat. Commun.* **2023**, *14*, 6733.
6 Lei, W. W.; Suzuki, N.; Terashima, C.; Fujishima, A. Hydrogel photocatalysts for efficient energy conversion and environmental treatment. *Front. Energy* **2021**, *15*, 577–595.
7 Kumar, N.; Gusain, R.; Pandey, S.; Ray, S. S. Hydrogel nanocomposite adsorbents and photocatalysts for sustainable water purification. *Adv. Mater. Interfaces* **2023**, *10*, 2201375.
8 Esen, C.; Kumru, B. Photocatalyst-incorporated cross-linked porous polymer networks. *Ind. Eng. Chem. Res.* **2022**, *61*, 10616–10630.
9 Li, Q. Q.; Zhao, C. Z.; Jia, S. S.; Chen, Q.; Li, X. S.; She, M. Y.; Liu, H.;

Graphical Abstract

Engineering Hydrogel-based Self-floating Catalytic Materials for Interfacial Solar-driven Chemistry

Jia-Xin Gao and Wen-Wei Lei

Yanshan University

This review highlights hydrogel-based self-floating catalysts as innovative interfacial platforms for solar-driven chemistry. By establishing stable three-phase interfaces, these materials overcome traditional mass-transfer limitations and catalyst agglomeration. We analyze core construction strategies and demonstrate their versatile applications in pollutant degradation, hydrogen production, and desalination.

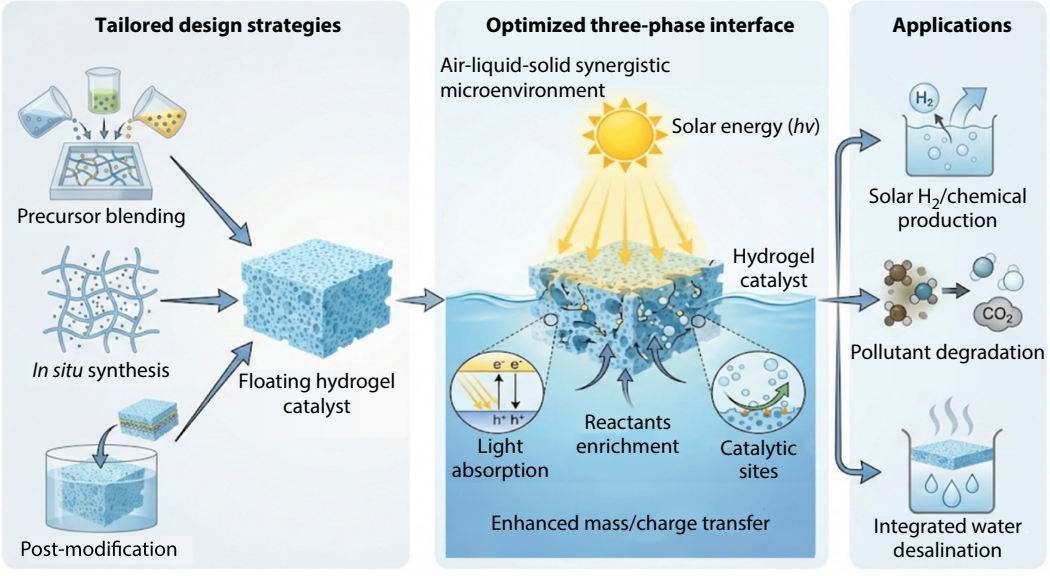

Chinese J. Polym. Sci. 2026, 44, 1695–1715 *https://doi.org/10.1007/s10118-026-3578-9*

Liu, P.; Wang, Y. Y.; Li, J. L. Design and fabrication of Cu Ⅰ/Cu Ⅱ-MOF-incorporated hydrogel photocatalysts for synergy removal of Cr(IV) and congo red. *Chin. Chem. Lett.* **2025**, *36*, 109936.
10 Su, J. Q.; Wang, P. J.; Zhou, W.; Peydayesh, M.; Zhou, J. T.; Jin, T. H.; Donat, F.; Jin, C. Y.; Xia, L.; Wang, K. W.; Ren, F. Z.; Van der Meeren, P.; de Arquer, F. P. G.; Mezzenga, R. Single-site iron-anchored amyloid hydrogels as catalytic platforms for alcohol detoxification. *Nat. Nanotechnol.* **2024**, *19*, 1168–1177.
11 Zhou, H.; Sheng, X.; Xiao, J.; Ding, Z. Y.; Wang, D. D.; Zhang, X. Q.; Liu, J.; Wu, R. F.; Feng, X. J.; Jiang, L. Increasing the efficiency of photocatalytic reactions *via* surface microenvironment engineering. *J. Am. Chem. Soc.* **2020**, *142*, 2738–2743.
12 Huang, H. N.; Shi, R.; Zhang, X. R.; Zhao, J. Q.; Su, C. L.; Zhang, T. R. Photothermal-assisted triphase photocatalysis over a multifunctional bilayer paper. *Angew. Chem. Int. Ed.* **2021**, *60*, 22963–22969.
13 Fu, J. C.; Xiao, S. Z.; Cao, J. Z.; Liang, Z. Y.; Chen, J. B.; Jiang, Y.; Xing, M. Y. Mass transfer-enhanced photothermal membranes with synergistic light utilization for high-turbidity wastewater purification. *Angew. Chem. Int. Ed.* **2025**, *64*, e202421800.
14 Ju, Y. J.; Li, H.; Wang, Z.; Liu, H. W.; Huo, S. H.; Jiang, S.; Duan, S. C.; Yao, Y. G.; Lu, X. Q.; Chen, F. J. Solar-driven on-site H_2O_2 generation and tandem photo-Fenton reaction on a triphase interface for rapid organic pollutant degradation. *Chem. Eng. J.* **2022**, *430*, 133168.
15 Jiang, M. P.; Li, J. J.; Wan, X. Y.; Qiu, J. H.; Yao, T. T.; Zhang, W. Y.; Ma, S. Y.; Tan, H.; Han, A.; Chen, C. L.; Liu, G. Floatable organic-inorganic hybrid-TiO_2 unlocks superoxide radicals for plastic photoreforming in neutral solution. *Nat. Commun.* **2025**, *16*, 4136.
16 Wu, T.; Liang, Q. H.; Tang, L.; Tang, J. L.; Wang, J. J.; Shao, B. B.; Gong, S. X.; He, Q. Y.; Pan, Y.; Liu, Z. F. Construction of a novel S-scheme heterojunction piezoelectric photocatalyst S-$BiOIO_3$/FTCN and immobilization with floatability for tetracycline degradation. *J. Hazard. Mater.* **2023**, *443*, 130251.
17 He, B. W.; Wang, Z. L.; Xiao, P.; Chen, T.; Yu, J. G.; Zhang, L. Y. Cooperative coupling of H_2O_2 production and organic synthesis over a floatable polystyrene-sphere-supported TiO_2/Bi_2O_3 S-scheme photocatalyst. *Adv. Mater.* **2022**, *34*, 2203225.
18 Liu, X. Y.; Pan, J. A.; Huang, H.; Sun, N.; Gu, C.; Zhuang, Y. L.; Wang, L. L. Floating solar materials and their devices for energy conversion and environment remediation. *Adv. Sustain. Syst.* **2024**, *8*, 2400118.
19 Guo, Y. X.; Dong, Y. M.; Liu, B.; Ni, B. Q.; Pan, C. S.; Zhang, J. W.; Zhao, H.; Wang, G. L.; Zhu, Y. F. Effective H_2O_2 photosynthesis in gas-liquid-solid triphase system with self-floating conjugated organic polymers. *Adv. Funct. Mater.* **2024**, *34*, 2402920.
20 Wang, J.; Zhang, J. H.; Li, Y.; Xia, X. H.; Yang, H. J.; Kim, J. H.; Zhang, W. Silver single atoms and nanoparticles on floatable monolithic photocatalysts for synergistic solar water disinfection. *Nat. Commun.* **2025**, *16*, 981.
21 Sahoo, L.; Mondal, S.; Beena, N. C.; Gloskovskii, A.; Manju, U.; Topwal, D.; Gautam, U. K. 3D porous polymeric-foam-supported Pd nanocrystal as a highly efficient and recyclable catalyst for organic transformations. *ACS Appl. Mater. Interfaces* **2021**, *13*, 10120–10130.
22 Zha, Q. D.; Yin, Z. Z.; Yang, G. Y.; Wang, R. R.; Xie, Y.; Chen, Y. H.; Hong, Z.; Luo, Y. D.; Xue, M. S. Unique biomimetic self-floating 3D janus 'integrated system' for efficient interfacial solar steam generation and wastewater treatment. *Sep. Purif. Technol.* **2025**, *372*, 133439.
23 Zhang, Z.; Zhang, L.; Huang, Z. H.; Xu, Y. X.; Zhao, Q. Q.; Wang, H. J.; Shi, M. Q.; Li, X. N.; Jiang, K.; Wu, D. P. "Floating catalytic foam" with prominent heat-induced convection for the effective photocatalytic removal of antibiotics. *J. Hazard. Mater.* **2024**, *463*, 132879.
24 Wang, J. M.; Jiang, J. Z.; Li, F. Y.; Zou, J.; Xiang, K.; Wang, H. T.; Li, Y. J.; Li, X. Emerging carbon-based quantum dots for sustainable photocatalysis. *Green Chem.* **2023**, *25*, 32–58.
25 Hu, Z. F.; Shen, Z. R.; Yu, J. C. Converting carbohydrates to carbon-based photocatalysts for environmental treatment. *Environ. Sci. Technol.* **2017**, *51*, 7076–7083.
26 He, Y. M.; Li, H. Y.; Guo, X. L.; Zheng, R. B. Bleached wood supports for floatable, recyclable, and efficient three dimensional photocatalyst. *Catalysts* **2019**, *9*, 115.
27 Li, W.; Chen, Z. J.; Yu, H. P.; Li, J.; Liu, S. X. Wood-derived carbon materials and light-emitting materials. *Adv. Mater.* **2021**, *33*, 2000596.
28 An, N.; Zhang, X.; Chen, Y.; Wang, Z. N.; Qiu, J. S.; Gao, B. Y.; Li, Q. A self-floating photothermal/photocatalytic evaporator for simultaneous high-efficiency evaporation and purification of volatile organic wastewater. *Adv. Funct. Mater.* **2025**, *35*, 2500777.
29 Chi, W. W.; Dong, Y. M.; Liu, B.; Pan, C. S.; Zhang, J. W.; Zhao, H.; Zhu, Y. F.; Liu, Z. Y. A photocatalytic redox cycle over a polyimide catalyst drives efficient solar-to-H_2O_2 conversion. *Nat. Commun.* **2024**, *15*, 5316.
30 Yang, J. M.; Lu, J. L.; Han, D. X.; Zhou, B.; Du, A. Direct ink writing of aerogels: Fundamentals, strategies, applications, and perspectives. *Prog. Mater. Sci.* **2025**, *152*, 101462.
31 Xing, C. Y.; Li, Z. H.; Wang, Z.; Zhang, S. H.; Xie, Z. J.; Zhu, X.; Peng, Z. C. Chemical scissors tailored nano-tellurium with high-entropy morphology for efficient foam-hydrogel-based solar photothermal evaporators. *Nano-Micro Lett.* **2024**, *16*, 47.
32 Hou, L. H.; Xing, Z. Z.; Luo, S. J.; Li, T. L.; Wang, H. T. Self-regulating hydrogel spheres for salt-resistant solar desalination. *Desalination* **2025**, *615*, 119255.
33 Wang, Y. M.; Fang, J. W.; Li, S. H.; Luo, S. Y.; Mo, C. N.; Qi, R. H. Floating beyond limits: a review on engineered floatable hydrogel platforms and emerging sustainable applications. *Renew. Sust. Energ. Rev.* **2025**, *219*, 115880.
34 Fan, G. D.; Du, B. H.; Zhou, J. J.; Yan, Z. S.; You, Y. F.; Luo, J. Porous self-floating 3D Ag_2O/g-C_3N_4 hydrogel and photocatalytic inactivation of microcystis aeruginosa under visible light. *Chem. Eng. J.* **2021**, *404*, 126509.
35 Wang, X.; Wang, Q. G. Enzyme-laden bioactive hydrogel for biocatalytic monitoring and regulation. *Acc. Chem. Res.* **2021**, *54*, 1274–1287.
36 Zhu, X. Y.; Zhang, L. H.; Zou, G. L.; Chen, Q.; Guo, Y. L.; Liang, S. M.; Hu, L. J.; North, M.; Xie, H. B. Carboxylcellulose hydrogel confined-Fe_3O_4 nanoparticles catalyst for Fenton-like degradation of rhodamine B. *Int. J. Biol. Macromol.* **2021**, *180*, 792–803.
37 Yang, W. J.; Si, L. F.; Cheng, C.; Cui, Y. Y.; Yan, X. L.; Liu, M. C.; Jing, D. W.; Shi, J. W.; Guo, L. J. Synergistic integration of atmospheric water harvesting and solar-driven hydrogen production *via* multifunctional hygroscopic-photocatalytic hydrogel nanocomposite. *Adv. Funct. Mater.* **2026**, *36*, e12738.
38 Liu, M.; Li, Y. X.; Liu, B. Z.; Li, L. K.; Guo, X.; Wu, Y. Q. CNF@Fe^{3+}-PEDOT: PSS/$CuCo_2O_4$ hydrogel enabling coupled photocatalysis-PMS activation-Fe^{3+}/Fe^{2+} redox shuttle for durable antibiotic removal. *Appl. Catal. B-Environ. Energy* **2026**, *382*, 126026.
39 He, H.; Zhang, Q.; Zhang, Y. M.; Qu, S. X.; Li, B.; Lin, J.; Lu, X.; Xie, C. M. Injectable bioadhesive and lubricating hydrogel with polyphenol mediated single atom nanozyme for rheumatoid arthritis therapy. *Nat. Commun.* **2025**, *16*, 2768.
40 Zhu, D. M.; Chen, H.; Huang, C. Y.; Li, G. X.; Wang, X.; Jiang, W.; Fan, K. L. H_2O_2 self-producing single-atom nanozyme hydrogels

as light-controlled oxidative stress amplifier for enhanced synergistic therapy by transforming "cold" tumors. *Adv. Funct. Mater.* **2022**, *32*, 2110268.
41 Yan, H. Y.; Jiao, L.; Wang, H. J.; Zhu, Y. M.; Chen, Y. F.; Shuai, L.; Gu, M.; Qiu, M.; Gu, W. L.; Zhu, C. Z. Single-atom Bi-anchored au hydrogels with specifically boosted peroxidase-like activity for cascade catalysis and sensing. *Sens. Actuator B-Chem.* **2021**, *343*, 130108.
42 Byun, J.; Landfester, K.; Zhang, K. A. I. Conjugated polymer hydrogel photocatalysts with expandable photoactive sites in water. *Chem. Mat.* **2019**, *31*, 3381–3387.
43 Hu, X. L.; Zhan, Z.; Zhang, J. Q.; Hussain, I.; Tan, B. E. Immobilized covalent triazine frameworks films as effective photocatalysts for hydrogen evolution reaction. *Nat. Commun.* **2021**, *12*, 6596.
44 Kuckhoff, T.; Landfester, K.; Zhang, K. A. I.; Ferguson, C. T. J. Photocatalytic hydrogels with a high transmission polymer network for pollutant remediation. *Chem. Mat.* **2021**, *33*, 9131–9138.
45 An, N.; Su, R. D.; Wang, Z. N.; Chen, W. F.; Zhou, W. Z.; Li, Q. Hydrogel-based photothermal evaporator for efficient solar desalination and synergistic removal of volatile organic compounds. *Desalination* **2023**, *565*, 116849.
46 Jiao, Y. Y.; Cheng, Z. Y.; Luo, H.; Zhao, Q. P.; Xiang, X. Y.; Zhang, Z. M. Floatable Fe-TiO_2/hydrogel composite for photodegradation of water pollutants. *Sci. China-Mater.* **2024**, *67*, 4013–4020.
47 Kaur, K.; Jindal, R. Comparative study on the behaviour of chitosan-gelatin based hydrogel and nanocomposite ion exchanger synthesized under microwave conditions towards photocatalytic removal of cationic dyes. *Carbohydr. Polym.* **2019**, *207*, 398–410.
48 Kuspanov, Z.; Bakbolat, B.; Baimenov, A.; Issadykov, A.; Yeleuov, M.; Daulbayev, C. Photocatalysts for a sustainable future: Innovations in large-scale environmental and energy applications. *Sci. Total Environ.* **2023**, *885*, 163914.
49 Zhang, Y.; Liu, L. X.; Yin, S. X.; Zhou, C.; Ding, Y.; Che, G. J.; Zhao, C. Q. Underwater high strength and tough polyvinyl alcohol-polyacrylic acid hydrogel. *Adv. Funct. Mater.* **2025**, *35*, 2503023.
50 Zhang, Y. S.; Khademhosseini, A. Advances in engineering hydrogels. *Science* **2017**, *356*, eaaf3627.
51 Zhu, T. X.; Ni, Y. M.; Biesold, G. M.; Cheng, Y.; Ge, M. Z.; Li, H. Q.; Huang, J. Y.; Lin, Z. Q.; Lai, Y. K. Recent advances in conductive hydrogels: Classifications, properties, and applications. *Chem. Soc. Rev.* **2023**, *52*, 473–509.
52 Wang, Z. W.; Wei, H.; Huang, Y. J.; Wei, Y.; Chen, J. Naturally sourced hydrogels: Emerging fundamental materials for next-generation healthcare sensing. *Chem. Soc. Rev.* **2023**, *52*, 2992–3034.
53 Guo, Y. H.; Bae, J.; Fang, Z. W.; Li, P. P.; Zhao, F.; Yu, G. H. Hydrogels and hydrogel-derived materials for energy and water sustainability. *Chem. Rev.* **2020**, *120*, 7642–7707.
54 Zhao, F.; Bae, J.; Zhou, X. Y.; Guo, Y. H.; Yu, G. H. Nanostructured functional hydrogels as an emerging platform for advanced energy technologies. *Adv. Mater.* **2018**, *30*, 1801796.
55 Yang, Y. C.; Ru, Y. F.; Zhao, T. Y.; Liu, M. J. Bioinspired multiphase composite gel materials: From controlled micro-phase separation to multiple functionalities. *Chem* **2023**, *9*, 3113–3137.
56 Amalia, F. R.; Wang, L.; Bielan, Z.; Markowska-Szczupak, A.; Wei, Z. S.; Kowalska, E. Gels in heterogeneous photocatalysis: Past, present, and future. *Gels* **2024**, *10*, 810.
57 Sun, J.; Wang, L. X.; Huang, T.; Liu, K.; Fu, T.; Xu, Z. S.; Yang, W. H.; Tong, Z. F.; Zhang, H. B. Floating BiOBr/Ti_3C_2 aerogel spheres for efficient degradation of quinolone antibiotics: Rapid oxygen transfer *via* triphase interface and effective charges separation by internal electric field. *J. Colloid Interface Sci.* **2025**, *685*, 813–825.
58 Wu, Y. C.; Zhang, L. Q.; Ge, J. L.; Zhang, Y. T.; Liu, L. Y.; Lan, Q. Q.; Liu, T. X. Phenolic aerogels with gradient porosity and self-floating photothermal interface for seawater desalination and wastewater purification. *Desalination* **2024**, *586*, 117771.
59 Zhang, L. H.; Yan, H.; Zhou, J. J.; Zhao, Z. G.; Huang, J.; Chen, L.; Ru, Y. F.; Liu, M. J. High-performance organohydrogel artificial muscle with compartmentalized anisotropic actuation under microdomain confinement. *Adv. Mater.* **2023**, *35*, 2202193.
60 Zhang, L. X.; Rao, L.; Wang, P. F.; Shi, Z. Y.; Wang, P. F. Superhydrophobic self-floating TiO_2-silicone composite aerogels and their air-liquid-solid triphase photocatalytic system. *Appl. Surf. Sci.* **2021**, *536*, 147726.
61 Wang, K.; Zhao, T.; Ren, N. Q.; Ho, S. H. Asymmetric defective sites-mediated high-valent cobalt-oxo species in self-suspension aerogel platform for efficient peroxymonosulfate activation. *Water Res.* **2024**, *265*, 122304.
62 Yao, D. C.; Chen, Z.; Chu, C. C.; Ran, X. M.; Liu, X. R.; Mao, S. Positionally isomeric conjugated polymers for photosynthesis of hydrogen peroxide through triphase interface reaction. *Appl. Catal. B-Environ. Energy* **2025**, *367*, 125071.
63 Lei, L.; Wang, W. J.; Wang, C.; Fan, H. Q.; Yadav, A. K.; Hu, N.; Zhong, Q.; Müller-Buschbaum, P. Hydrogel-supported graphitic carbon nitride nanosheets loaded with Pt atoms as a novel self-water-storage photocatalyst for H_2 evolution. *J. Mater. Chem. A* **2020**, *8*, 23812–23819.
64 Jiang, W. J.; Luo, W. J.; Zong, R. L.; Yao, W. Q.; Li, Z. P.; Zhu, Y. F. Polyaniline/Carbon Nitride nanosheets composite hydrogel: a separation-free and high-efficient photocatalyst with 3D hierarchical structure. *Small* **2016**, *12*, 4370–4378.
65 Sharma, G.; Kumar, A.; Sharma, S.; Al-Muhtaseb, A. H.; Naushad, M.; Ghfar, A. A.; Ahamad, T.; Stadler, F. J. Fabrication and characterization of novel Fe^0@Guar gum-crosslinked-soya lecithin nanocomposite hydrogel for photocatalytic degradation of methyl violet dye. *Sep. Purif. Technol.* **2019**, *211*, 895–908.
66 Wang, J. M.; Li, X. X.; Cheng, Q. Y.; Lv, F. Z.; Chang, C. Y.; Zhang, L. N. Construction of β-FeOOH@tunicate cellulose nanocomposite hydrogels and their highly efficient photocatalytic properties. *Carbohydr. Polym.* **2020**, *229*, 115470.
67 Hu, C.; Lin, Y. R.; Yang, H. C. Recent developments in graphitic Carbon Nitride based hydrogels as photocatalysts. *ChemSusChem* **2019**, *12*, 1794–1806.
68 Jiang, W. J.; Zhu, Y. F.; Zhu, G. X.; Zhang, Z. J.; Chen, X. J.; Yao, W. Q. Three-dimensional photocatalysts with a network structure. *J. Mater. Chem. A* **2017**, *5*, 5661–5679.
69 Wen, Y. T.; Xue, C. L.; Ji, D. L.; Zhang, Y.; Zhang, M.; Gong, W. Q.; Li, Z. Q.; Li, Y. Green construction of self-floating polysaccharide-based hydrogels with catalytic activity for efficient organic pollutants reduction. *Int. J. Biol. Macromol.* **2024**, *271*, 132507.
70 Chen, W.; Liu, Z. Z.; Xie, Y. S.; Guo, X. Z.; Xie, H. J.; Chen, J. H.; Zhang, Z.; Ding, L. Synthesis of ZIF-67 composite lignin hydrogel and its catalytic degradation of naphthalene by PMS in wastewater. *Int. J. Biol. Macromol.* **2025**, *298*, 139700.
71 Wang, F.; Zhang, Y. R.; Peng, Y. Y.; Xiao, W. Y.; Yu, W. C.; Wang, H.; Bian, Z. Y. Continuous peroxymonosufate activation for antibiotics degradation *via* Fluorine-free-$Ti_3C_2T_x$-$CoFe_2O_4$ hydrogel beads: Performance, mechanism and application. *Appl. Catal. B-Environ. Energy* **2024**, *358*, 124441.
72 Zhou, H. S.; Zha, H.; Zhang, Z. Z.; Huang, J.; Liu, M. J. Advanced mechanical polymer nanocomposites: From confined interphase to structural synergy. *Chem. Commun.* **2025**, *61*, 16132–16149.
73 Chen, L.; Chai, J.; Zhang, L.; Zhou, J.; Huang, J.; Liu, M. High-

strength shape-memory ionogels with controllable metastable state for high-work-density actuation. *CCS Chem.* **2025**, *7*, 2086–2097.
74 Tang, Y. A.; Qin, Z.; Zhong, Y. H.; Yin, S. Y.; Liang, S.; Sun, H. Three-phase interface photocatalysis for the enhanced degradation and antibacterial property. *J. Colloid Interface Sci.* **2022**, *612*, 194–202.
75 Mohapatra, L.; Paramanik, L.; Sabnam, S.; Yoo, S. H. Advanced strategies for controlling three-phase boundaries in photocatalysis. *Nanoscale* **2024**, *16*, 22099–22119.
76 Mu, C. F.; Zhang, Y.; Cui, W. Q.; Liang, Y. H.; Zhu, Y. F. Removal of bisphenol a over a separation free 3D Ag_3PO_4-graphene hydrogel *via* an adsorption-photocatalysis synergy. *Appl. Catal. B-Environ.* **2017**, *212*, 41–49.
77 Li, J. Y.; Yu, X.; Zhu, Y.; Fu, X. H.; Zhang, Y. M. 3D-2D-3D BiOI/porous g-C_3N_4/graphene hydrogel composite photocatalyst with synergy of adsorption-photocatalysis in static and flow systems. *J. Alloy. Compd*. **2021**, *850*, 156778.
78 Yang, J. H.; Li, Z. K.; Zhu, H. J. Adsorption and photocatalytic degradation of sulfamethoxazole by a novel composite hydrogel with visible light irradiation. *Appl. Catal. B-Environ.* **2017**, *217*, 603–614.
79 Li, Y.; Cui, W. Q.; Liu, L.; Zong, R. L.; Yao, W. Q.; Liang, Y. H.; Zhu, Y. F. Removal of Cr(Ⅵ) by 3D TiO_2-graphene hydrogel *via* adsorption enriched with photocatalytic reduction. *Appl. Catal. B-Environ.* **2016**, *199*, 412–423.
80 Yin, S. X.; Ding, Y.; Zhang, Y.; Zhou, C.; Qian, C.; Che, G. J.; Zhao, C. Q.; Jiang, L. Superstrong and transparent hydrogels with homogeneous multiple networks. *Macromolecules* **2025**, *58*, 4357–4364.
81 Dalponte, I.; de Sousa, B. C.; Mathias, A. L.; Jorge, R. M. M. Formulation and optimization of a novel TiO_2/calcium alginate floating photocatalyst. *Int. J. Biol. Macromol.* **2019**, *137*, 992–1001.
82 Gou, K. J.; Li, T. X.; Zhang, C. Y.; Wu, D. X.; Zhu, H. T. Salting-out/sacrificial template strategy for the preparation of hydrogels as efficient solar evaporators. *Chem. Eng. J.* **2024**, *480*, 148210.
83 Wang, Y.; Chai, J.; Wang, H.; Xiao, T.; Zhao, J.; Chen, L.; Lei, W.; Liu, M. Solvent-mediated microphase separation in ionogels for the construction of mechanically robust and high-energy-output moisture-electric generators. *Interdisciplinary Mater.* **2025**, *4*, 869–880.
84 Yang, X.; Shi, F.; Su, X. L.; Cavaco-Paulo, A.; Wang, H. B.; Su, J. In-situ encapsulation and construction of Lac@HOFs/hydrogel composite for enhancing laccase stability and azo dyes decolorization efficiency. *Carbohydr. Polym.* **2023**, *320*, 121157.
85 Li, S. M.; Liu, J.; Li, C. J.; Fang, X. Y.; Wang, X.; Tian, L.; Yu, Z. Z.; Li, X. F. Robust and antifouling composite hydrogels enhanced by directional freeze-casting and salting-out for highly efficient solar evaporation. *ACS Appl. Mater. Interfaces* **2024**, *16*, 66560–66570.
86 Zhang, X. T.; Chen, W. L.; Li, X. Q. Efficiently recyclable Fe-doped ZnO/bacterial cellulose-based composite aerogel for photocatalytic degradation of methylene blue under visible light. *J. Polym. Environ.* **2024**, *32*, 4315–4329.
87 Ren, J. X.; Zhu, J. L.; Shi, S. C.; Yin, M. Q.; Huang, H. D.; Li, Z. M. In-situ structuring a robust cellulose hydrogel with ZnO/SiO_2 heterojunctions for efficient photocatalytic degradation. *Carbohydr. Polym.* **2022**, *296*, 119957.
88 Ahmadian, Z.; Kazeminava, F.; Afrouz, M.; Abbaszadeh, M.; Mehr, N. T.; Shiran, J. A.; Gouda, C.; Adeli, M.; Kafil, H. S. A review on the impacts of metal/metal nanoparticles on characteristics of hydrogels: Special focus on carbohydrate polymers. *Int. J. Biol. Macromol.* **2023**, *253*, 126535.
89 Lin, L.; Wang, W. R.; Li, D. Y.; Xu, S. Y.; Sun, Y.; Li, L. F.; Fan, K.; Xing, C. Y.; Zhang, L.; Li, J. H. Multifunctional graphene/Ag hydrogel with antimicrobial and catalytic properties for efficient solar-driven desalination and wastewater purification. *Chem. Eng. J.* **2023**, *478*, 147249.
90 Nayak, S.; Goswami, S.; Sharma, D.; Sen, A.; Sarkar, A.; Naskar, D.; Dan, A. In-situ grown nanosilver in chitosan-graphene oxide hydrogels as a robust composite catalyst for sustainable degradation of organic water pollutants. *Int. J. Biol. Macromol.* **2025**, *330*, 147952.
91 Lan, L. M.; Liu, B. N.; Li, W. X.; Bu, H. T.; Hu, T.; Hu, H. J.; Li, Y. T.; Jiang, G. B. Facilely recoverable Pb(Ⅱ) adsorbent based on greigite (Fe_3S_4) loaded alginate aerogel with high adsorption efficiency. *Chemosphere* **2022**, *290*, 133264.
92 Zhao, H.; Li, Y. Removal of heavy metal ion by floatable hydrogel and reusability of its waste material in photocatalytic degradation of organic dyes. *J. Environ. Chem. Eng.* **2021**, *9*, 105316.
93 Ding, N.; Zhu, J.; Qiao, Y.; Yao, D.; Gao, X.; Chen, J.; Lu, C.; Pang, X. Janus-structured self-floating hydrogel *via* thermal localization and arched evaporation interface design toward all-weather efficient solar desalination. *Chem. Eng. J.* **2025**, *513*, 162851.
94 Han, M. Z.; Wang, Z. H.; Xie, Z. Y.; Hou, M. X.; Gao, Z. P. Polydopamine-modified sodium alginate hydrogel for microplastics removal: adsorption performance, characteristics, and kinetics. *Int. J. Biol. Macromol.* **2025**, *297*, 139947.
95 Shen, F. T.; Wang, J. Z.; Wang, L. B.; Zang, L. L.; Xu, Q.; Sun, L. G.; Zhang, Y. H. Copper phthalocyanine modified hydrogel inverse opal beads for enhanced photocatalytic removal of dyes. *J. Mater. Chem. A* **2023**, *11*, 10195–10203.
96 Zhou, S. Y.; Ren, Z. Y.; Yang, L.; Zhu, C. L.; Xie, W. X.; Feng, X. Y.; Jing, Q. *In situ* anchoring of Fe-doped ZIF-67 on nanocellulose/chitosan aerogel for efficient removal of tetracycline: synergistic effects of adsorption and catalysis. *J. Environ. Chem. Eng*. **2025**, *13*, 119954.
97 Wang, Y.; Qin, H.; Li, Z.; Dai, J.; Cong, H.-P.; Yu, S.-H. Highly compressible and environmentally adaptive conductors with high-tortuosity interconnected cellular architecture. *Nature Synthesis* **2022**, *1*, 975–986.
98 Hou, Z. H.; Sun, Q.; Wang, Z. Y.; Bai, L. J.; Chen, H.; Wang, W. X.; Yang, L. X.; Yang, H. W.; Wei, D. L. Fabrication of amphoteric gelatin nanospheres-doped self-healing nanocomposite hydrogels and the application in flexible sensors. *React. Funct. Polym.* **2023**, *192*, 105729.
99 Lei, W. W.; Liu, Y. H.; Khan, S.; Suzuki, N.; Terashima, C.; Fujishima, A.; Liu, M. J. Synergistically regulated surface structure and water transportation of sponge hydrogel evaporator for efficient water desalination. *Desalination* **2022**, *533*, 115780.
100 Li, N.; Luo, L.; Guo, C.; He, J. T.; Wang, S. X.; Yu, L. M.; Wang, M.; Murto, P.; Xu, X. F. Shape-controlled fabrication of cost-effective, scalable and anti-biofouling hydrogel foams for solar-powered clean water production. *Chem. Eng. J.* **2022**, *431*, 134144.
101 Chen, L.; Ding, Y.; Gong, J.; Xie, H.; Qu, J. P.; Niu, R. Molecular engineering of biomass-derived hybrid hydrogels for solar water purification. *J. Colloid Interface Sci.* **2022**, *626*, 231–240.
102 Liu, W. Q.; Erol, O.; Gracias, D. H. 3D printing of an *in situ* grown mof hydrogel with tunable mechanical properties. *ACS Appl. Mater. Interfaces* **2020**, *12*, 33267–33275.
103 Zhu, J.; Xiao, Z. Y.; Song, F. Y.; Huang, X. Y.; Chen, D. Y.; Nie, Z. H. Amphiphilic janus patch-grafted hydrogels for salt-rejecting solar water desalination. *J. Mater. Chem. A* **2024**, *12*, 17142.
104 Lin, X. L.; Wang, P.; Hong, R. T.; Zhu, X.; Liu, Y. C.; Pan, X. J.; Qiu, X. Q.; Qin, Y. L. Fully lignocellulosic biomass-based double-layered

porous hydrogel for efficient solar steam generation. *Adv. Funct. Mater.* **2022**, *32*, 2209262.
105 Tripathy, H.; Balakrishnan, A.; Chinthala, M.; Kumar, A. Ternary indium sulfide based 3D hydrogels as versatile photocatalysts: Unraveling peroxymonosulfate activation for sulfamethoxazole degradation and H_2O_2 production. *Ind. Eng. Chem. Res.* **2024**, *63*, 20125–20143.
106 Li, X. K.; Yang, R.; Zou, L.; Zheng, S. Z.; Chen, M. S.; Wen, J.; Zhang, H.; Wu, C.; Zhang, Y. C.; Zhou, Y. T. Reassessing the role of thermal convection in simultaneous water production and pollutant degradation in interfacial photothermal-photocatalytic systems. *Adv. Mater.* **2025**, *37*, 2416283.
107 Liu, C.; Yao, A. R.; Li, W.; Xu, Q.; Yang, L.; Ge, Y. Q.; Lan, J. W.; Lin, S. J.; Qiu, J. H. Design of Go@TiO_2 and PDA@CNC decorated gelatin aerogel for efficient adsorption and photocatalytic degradation of organic pollutants. *J. Water Process. Eng.* **2025**, *75*, 108024.
108 Sarkodie, B.; Amesimeku, J.; Frimpong, C.; Howard, E. K.; Feng, Q.; Xu, Z. Z. Photocatalytic degradation of dyes by novel electrospun nanofibers: a review. *Chemosphere* **2023**, *313*, 137654.
109 Amornpitoksuk, P.; Kongseng, P.; Chantarak, S.; Suwanboon, S. Degradation of organic pollutants by floatable Fe-PAM hydrogel. *Desalination* **2024**, *571*, 117103.
110 Suryaa, K. V.; Balakrishnan, A.; Chinthala, M.; Devi, K. B.; Tripathy, H.; Kumar, A.; Aminabhavi, T. M.; Rtimi, S. Photocatalytic self-Fenton degradation of tetracycline over Z-scheme functionalized g-C_3N_4/CeO_2/Bi_2S_3 hydrogel beads: dynamics, mechanism, degradation pathways and toxicity analysis. *Chem. Eng. J.* **2025**, *505*, 159470.
111 An, W. J.; Yang, T.; Liu, C.; Hu, J. S.; Cui, W. Q.; Liang, Y. H. $CuBi_2O_4$ surface-modified three-dimensional graphene hydrogel adsorption and *in situ* photocatalytic Fenton synergistic degradation of organic pollutants. *Appl. Surf. Sci.* **2023**, *615*, 156396.
112 Zhang, S. B.; Wang, X.; Shen, H. X.; Zhang, J.; Dong, W. L.; Yu, Z. Y. Scalable nanoplastic degradation in water with enzyme-functionalized porous hydrogels. *J. Hazard. Mater.* **2025**, *487*, 137196.
113 Lee, W. H.; Lee, C. W.; Cha, G. D.; Lee, B. H.; Jeong, J. H.; Park, H.; Heo, J.; Bootharaju, M. S.; Sunwoo, S. H.; Kim, J. H.; Ahn, K. H.; Kim, D. H.; Hyeon, T. Floatable photocatalytic hydrogel nanocomposites for large-scale solar hydrogen production. *Nat. Nanotechnol.* **2023**, *18*, 754–762.
114 He, C.; Shang, L.; Zhu, H. F.; Yu, L. C.; Wang, L. Z.; Zhang, J. L. Photocatalytic conversion of methane to ethanol at a three-phase interface with concentration-matched hydroxyl and methyl radicals. *J. Am. Chem. Soc.* **2024**, *146*, 11968–11977.
115 Yang, Y. Y.; Luo, T. T.; He, M.; Yu, J.; Wu, X.; An, M. Z.; Lei, T.; Qin, Q. Q.; Qin, S. H. Boosting hydroxyl radical production *via* floatable S-scheme heterojunction-integrated polyacrylic acid hydrogels as a photo-self-Fenton catalyst for pollutant removal. *J. Mater. Chem. A* **2025**, *13*, 14372–14391.
116 Li, Y. Z.; Chen, B. S.; Yao, D. H.; Gao, X. P.; Chen, J.; Lu, C.; Pang, X. C. Enhancing salt resistance and all-day efficient solar interfacial evaporation of antibacterial sodium alginate-based porous hydrogels *via* surface patterning. *Carbohydr. Polym.* **2025**, *359*, 123588.
117 Xu, X. Y.; Qiu, J. X.; Li, Z.; Fu, A. N.; Yuan, S. T.; Li, H.; Lu, B. Y. A bifunctional polyacrylamide-alginate-TiO_2 hydrogel solar evaporator for integrated high-efficiency desalination and photocatalytic degradation. *Desalination* **2025**, *611*, 118920.
118 Niu, R.; Ren, J. X.; Koh, J. J.; Chen, L.; Gong, J.; Qu, J. P.; Xu, X. D.; Azadmanjiri, J.; Min, J. K. Bio-inspired sandwich-structured all-day-round solar evaporator for synergistic clean water and electricity generation. *Adv. Energy Mater.* **2023**, *13*, 2302451.

https://doi.org/10.1007/s10118-026-3578-9